extracellular matrix separating tubules in the cortical area, excluding the subcapsular area [7].

Vascular system

Vasculitis is defined by the presence of leukocytic inflammation in the vessel wall with reactive damage to mural structures [2, 20]. Vasculitis is usually found in the kidney, as well as in the systemic organs, including the lung, bronchus, nasal cavity, gastrointestinal tract, skin, nerve, and muscles in ANCA-positive patients. Standardized names and definitions of primary systemic vasculitis have been adopted from the Nomenclature of Systemic Vasculitis in the Chapel Hill Consensus Conference (CHCC) [2]. In this categorization made according to the size of the artery, large vessel vasculitis, medium-sized vessel vasculitis, and small vessel vasculitis were classified. Large vessel refers to the aorta and the largest branches directed toward major body regions; medium-sized vessel refers to the area from the main visceral arteries (e.g., renal, hepatic, coronary, and mesenteric arteries) to the distal arterial radicals that connect with arterioles. The vasculature of the kidney is composed of medium-sized arteries (renal artery, interlobar artery, arcuate artery, interlobular artery) and small vessels, including small-sized arteries (afferent arteriole, efferent arteriole), capillaries (glomerular capillary and peritubular capillary), and venules. ANCA-related vasculitis, such as WG, MPA, and CSS, typically affects small-vessel vasculitis, which shows histologically fibrinoid necrosis in the vessel wall [1]. By contrast, polyarteritis nodosa (PN), which is usually ANCA negative, is designated as vasculitis of medium-sized or small arteries without vasculitis in the glomerular capillaries and venules. However, some Japanese patients may also display MPO-ANCA (ANCA directed against myeloperoxidase as determined by ELISA), which reveals necrotizing vasculitis in medium-sized arteries without glomerular involvement (Fig. 12).

Fibrinoid necrosis

Necrotizing vasculitis showing fibrinoid necrosis in the interlobular artery (Fig. 13), or arteriole between the afferent artery and hilar artery (Fig. 14), or venule (Fig. 15) associated with few or no immune deposits is a common feature of WG, MPA, and CSS.

Granulomatous arteritis

According to CHCC, WG manifests with granulomatous arteritis, which reveals a palisading arrangement of infiltrating macrophages (palisade cells or epithelioid cells) surrounding a necrotic lesion, including multinucleated giant macrophages (Fig. 16a, b, c). This lesion should be differentiated from the reparative or healed granulation tissue stage of necrotizing vasculitis (Fig. 17a, b) [21].

Endarteritis

Endarteritis is reflected by arterial intimal proliferation, which may follow fibrinoid necrosis in the media, thereby inducing a narrowing of the artery with subsequent organ infarct or gut perforation. This lesion consists of proliferating myointimal cells, which are presumably derived from medial smooth muscle cells and can be found in fibrinoid-necrotizing medium-sized as well as small arteritis (Fig. 18). Myointimal cells with inflammatory cell infiltration result in fibrotic scar formation in the intima, a process known as occlusive endarteritis (Fig. 19), and can be potentiated by immunosuppressant therapy. In the EU-VAS scoring system, chronic endarteritis is designated as sclerosis [7].

Arteriosclerosis (arteriolosclerosis)

Arteriosclerosis (arteriolosclerosis) is defined as a chronic lesion characterized by abnormal thickening and hardening of the walls of the arteries with a loss of elasticity. The major form of arteriosclerosis in the medium-sized or small artery in the kidney does not show atherosclerosis, in which plaques of fatty deposits can be seen, but rather a proliferation of myointimal cells and fibroelastosis in the inner walls of the arteries (Fig. 20), by which arteriosclerosis may be distinguishable from endarteritis.

Histologic grading and staging of the glomerulointerstitial lesions in rapidly progressive nephritic syndrome (Shigematsu scoring system)

In Japan, one of the groups working on "Progressive Renal Diseases from the Specially Selected Diseases of the Ministry of Health and Welfare Research Project" (1996–1998) studied rapidly progressive nephritic syndrome (WHO) in an effort to develop earlier detection methods and to produce guidelines for the effective treatment of these syndromes [15]. Based on these efforts, histologic grading (acute activity index) and staging (chronicity index) for glomerular and interstitial lesions were developed by Shigematsu et al. to help to guide treatment decisions [16]. This histologic evaluation focused on the characterization of acute and chronic lesions among intracapillary, extracapillary, and interstitial lesions, as shown in Table 1. This system precisely assesses activity such as grading and chronicity as staging for glomerular lesions and interstitial lesions using a sum score in each

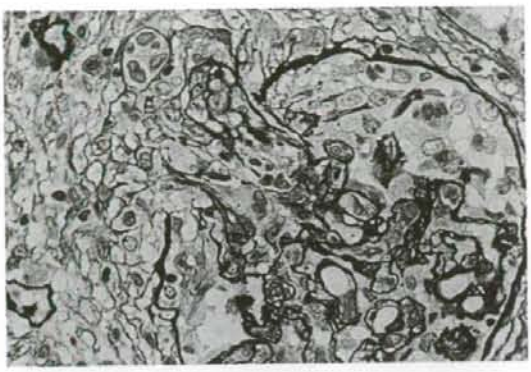

Fig. 14 Necrotizing vasculitis in an arteriole between the afferent artery and hilar artery in an MPO-ANCA-positive patient (PAM stain)

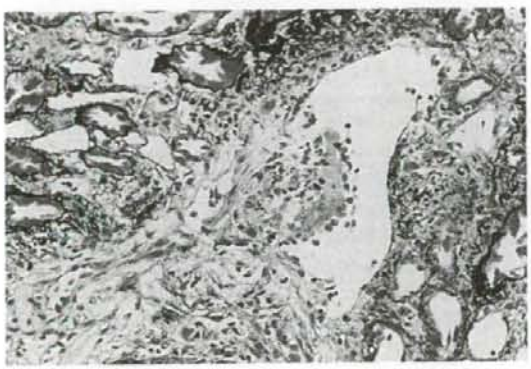

Fig. 15 Vasculitis in the venule of an MPO-ANCA-positive patient (PAM-Masson stain)

glomerular lesion, and then calculates a mean score by dividing the sum score by the total number of glomeruli [16]. However, this system is complicated and remains controversial for reproducibility, because the grades of the histological parameters are not expressed as an extent of distribution, but are expressed as the average number of grades and stages in respect to glomerular and tubulointerstitial lesions. Moreover, the vascular lesions were not considered histological parameters.

EUVAS histological classification

In the EUVAS scoring system, the severity of active as well as chronic histological parameters seen in the glomeruli are expressed as a percentage of the number of glomeruli showing a corresponding parameter to the total number of glomeruli. The histological parameter of the glomerulus includes fibrinoid tuft necrosis, extracapillary lesions (crescent), sclerosis, adhesion (synechia), and

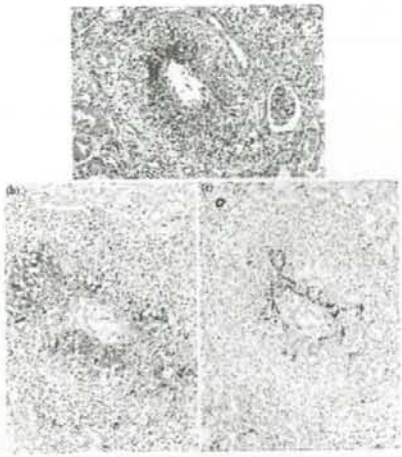

Fig. 16 Granulomatous arteritis of interlobular artery in an MPO-ANCA-positive patient. Granulomatous lesion showing palisading arrangement of the infiltrating macrophages (palisade cells), which surround a necrotic lesion, including multinucleated giant macrophages (**a**). Granulomatous lesion shows positive staining with anti-human macrophage antibody (KP1) (**b**), but negative staining for anti-smooth muscle actin, which stains only smooth muscle cells inside the artery (**c**). (**a** Masson stain, **b** immunoenzymatic method on a paraffin-embedded section using anti-human macrophage antibody (KP1), **c** immunoenzymatic method on a paraffin-embedded section using anti-smooth muscle actin)

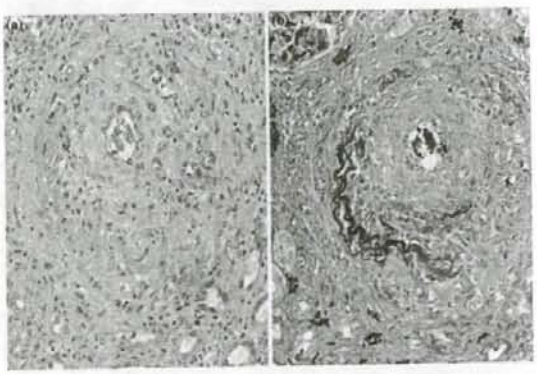

Fig. 17 Healed granulation tissue stage of necrotizing vasculitis (Arkin classification stage III) [21]. Arteritic lesion of interlobular artery in the kidney of a PN patient showing the healed granulation tissue stage in Arkin's classification (**a**) (HE stain). Elastica Masson staining shows the remaining internal elastic lamina (**b**)

others. Extracapillary lesions (crescent) are divided into circumferential (>50% of Bowman's space) and segmental (≤50% of Bowman's space), each of which is further divided into fibrous and cellular (including purely cellular and fibrocellular crescents) types. Among the number of each cellular or fibrous crescent, the numbers of crescentic glomeruli with periglomerular infiltrate and/or

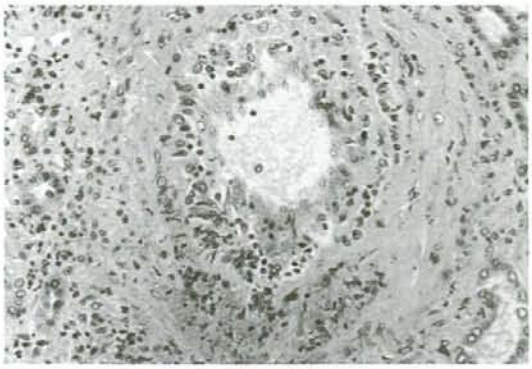

Fig. 18 Acute and active endarteritis of interlobular artery. Acute endarteritis consisting of proliferating myofibroblasts and inflammatory cells in the intima of medium-sized arteritis, which shows fibrinoid necrosis within the media (HE-stain)

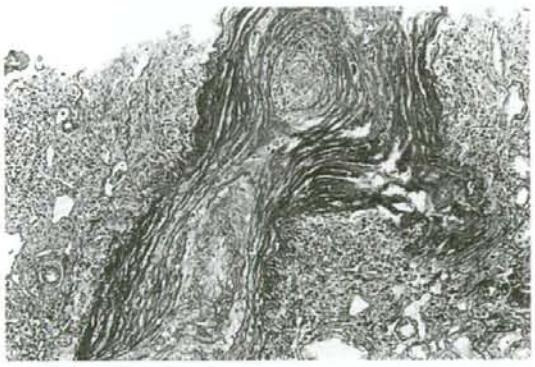

Fig. 19 Occlusive endarteritis of interlobular artery. Fibrotic scar with inflammatory cells in the intima results in arterial occlusion (PAM stain)

granulomatous reaction are calculated. Sclerosis is divided into local (small rounded area of scarring within the flocculus, <20% of the glomerulus), segmental (>20%, <80% of the glomerulus sclerosed within the flocculus), or global (>80% of the sclerosed glomerulus). Finally, among the local, segmental, and global sclerosis, the number of glomeruli with periglomerular infiltrate and granulomatous reactions is also calculated (Table 2).

Other parameters of the glomeruli are assessed dichotomously or trichotomously in the EUVAS scoring system, including mesangial proliferation [+ = more than three nuclei per peripheral mesangial area in glomeruli, which are not affected by sclerosis or extracapillary proliferation (score −/+)], mesangial matrix increase [significant increase of mesangial matrix in silver stain or PAS stain (score −/+], mononuclear/granular cell infiltration [significant: >5 cells per glomerulus in 50% of glomeruli,

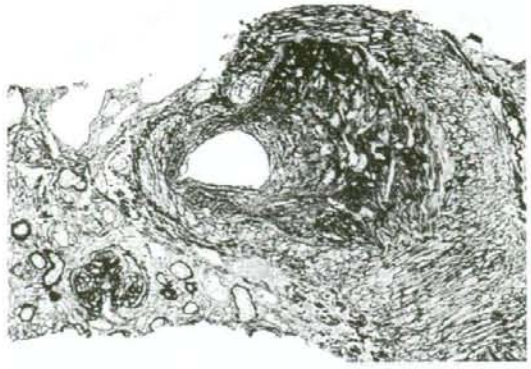

Fig. 20 Arteriosclerosis. The lesion in the medium-sized artery does not show fatty plaques, but does show proliferation of myofibroblasts and fibroelastosis in the inner walls of the arteries (PAM stain)

mononuclear cells or granulocytes in the capillary loops (including glomeruli affected by crescents or sclerosis), score + or −], and GBM thickening (thickening of the GBM, − = no thickening; + = thickening in <50% of the glomeruli; ++ = thickening in ≥50% of the glomeruli).

In evaluation of the tubulointerstitium by EUVAS, parameters including edema, focal infiltrates (− no infiltrate; + mild infiltrate; ++ dense infiltrate) or diffuse infiltrate (− no infiltrate; + mild infiltrate; ++ dense infiltrate), cell types of infiltrates (− = cell type is not present; + = cell type is present; ++ = cell type is predominantly present) for neutrophils, mononuclear cells, and eosinophils, fibrosis (− = no fibrosis; + = focal interstitial fibrosis; ++ = diffuse interstitial fibrosis), and interstitial granuloma (accumulation of epithelioid cells with or without giant cells without glomerular remnants (count the number of granuloma in the biopsy; may occur in perivascular, periglomerular and peritubular locations)).

In regard to the tubules, parameters included casts (− = no casts; + = occasional casts; ++ = numerous casts), necrosis − = absent; + = present), atrophy (− = absent, + = small foci or atrophy; ++ = extensive tubular atrophy), and intra-epithelial infiltration (infiltrate present in the tubular epithelium).

Parameters of arterial evaluation included sclerosis (intima fibrosis, splitting of elastica membrane, decrease of lumen size and/or calcification; score −/+), necrosis (presence of fibrin or fibrinoid material; score −/+), vessel wall infiltrate (score −/+), cell types of infiltrate (neutrophils, mononuclear cells, and eosinophils), vessel wall scaring, and thrombosis (score −/+/++).

In regard to the evaluation of arterioles, including afferent, efferent and medullar arterioles, parameters included hyalinosis (subendothelial deposits of PAS-positive material; score −/+), necrosis (score −/+/++), vessel wall infiltrate (score −/+), cell types of infiltrate

Table 1 Comparison of Shigematsu scoring system, EUVAS scoring system, and our proposal concerning histological parameters

Glomerulus	Shigematsu scoring	EUVAS scoring	Our proposal
Total number	○	○	○
Normal	○	○	○
Mesangial cell proliferation	×	○	○
Endocapillary hypercellularity	○	○	○
Tuft necrosis	○	○	○
Cellular/fibrocellular crescent	○	×	×
<50%	×	○	○
≥50%	×	○	○
Fibrous crescent	○	×	×
<50%	×	○	○
≥50%	×	○	○
Glomerulosclerosis			
Global	○	○	○
Segmental	○	○	○
Local	×	○	×
Collapse	○	×	○
Adhesion/synechia	○	○	○
Double contour	×	○	×
Destruction of Bowman's BM	○	×	○
Periglomerular infiltrate	×	○	×
Periglomerular granuloma	×	○	○
Fibrin thrombi	○	×	×
Mesangiolysis	○	×	×
Mesangial reticulation	○	×	×
Mesangial expansion	○	×	×
Mesangial interposition	○	×	×
Exudates into urinary space	○	×	×
Rupture of GBM	○	×	×
Extracapillary inflammatory cells	○	×	×
Parietal epithelial proliferation	○	×	×
Pseudotubularization	○	×	×
Ingrowth interstitium	○	×	×
Tubules			
Cast	×	○	×
Necrosis	×	○	○
Atrophy[a]	×	○	○
Intra-epithelial infiltrate (tubulitis)[a]	×	○	○
Destruction of tubular BM[a]	×	×	○
Interstitium			
Fibrosis	○	○	○
Infiltrate[a]			
Mononuclear cells	×	○	○
Neutrophils	×	○	○
Eosinophils	×	○	○
Granuloma	×	○	○
Edema	○	×	×
Peritubular capillaritis	○	×	○
Vascular			
Arcuate artery			
Sclerosis	×	×	○
Necrosis	×	×	○
Endarteritis	×	×	○
Cell type of infiltrate[a]			
Neutrophils	×	×	○
Mononuclear cells	×	×	○
Eosinophils	×	×	○
Thrombosis	×	○	○
Granulomatous change	×	×	○
Interlobular artery			
Sclerosis	×	○	○
Necrosis	×	○	○
Endarteritis	×	×	○
Cell type of infiltrate[a]			
Neutrophils	×	○	○
Mononuclear cells	×	○	○
Eosinophils	×	○	○
Thrombosis	×	○	○
Granulomatous change	×	×	○
Arteriole			
Hyalinosis	×	○	○
Necrosis	×	○	○
Cell type of infiltrate[a]			
Neutrophils	×	○	○
Mononuclear cells	×	○	○
Eosinophils	×	○	○
Thrombosis	×	○	○
Granulomatous change	×	×	○
Venular changes	×	×	○

[a] Evaluated by − non, + <25%; ++ 25–49%; +++ 50%≤

BM basement membrane

○ adopted

× unadopted

(neutrophils, mononuclear cells, and eosinophils), vessel wall scaring, and thrombosis (score −/+/++).

Proposal for standardization of pathological diagnosis

A score sheet for the proposed Japanese scoring system is included in Table 3. In addition to the parameters analyzed by the EUVAS systems, the present system also assesses

Table 2 EUVAS scoring system

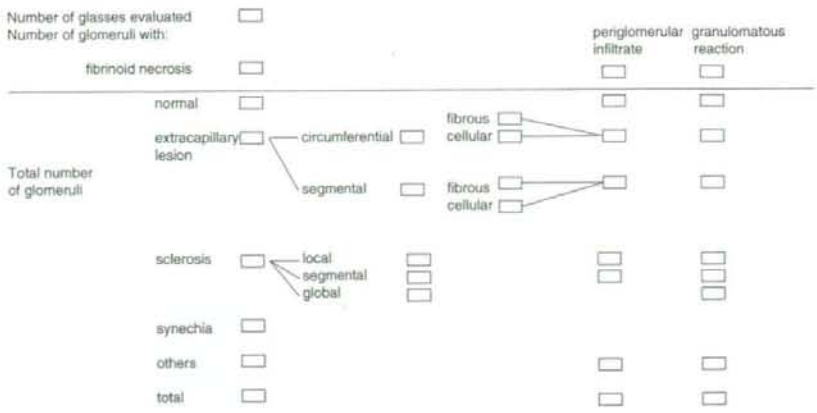

Table 3 Score sheet of our proposal

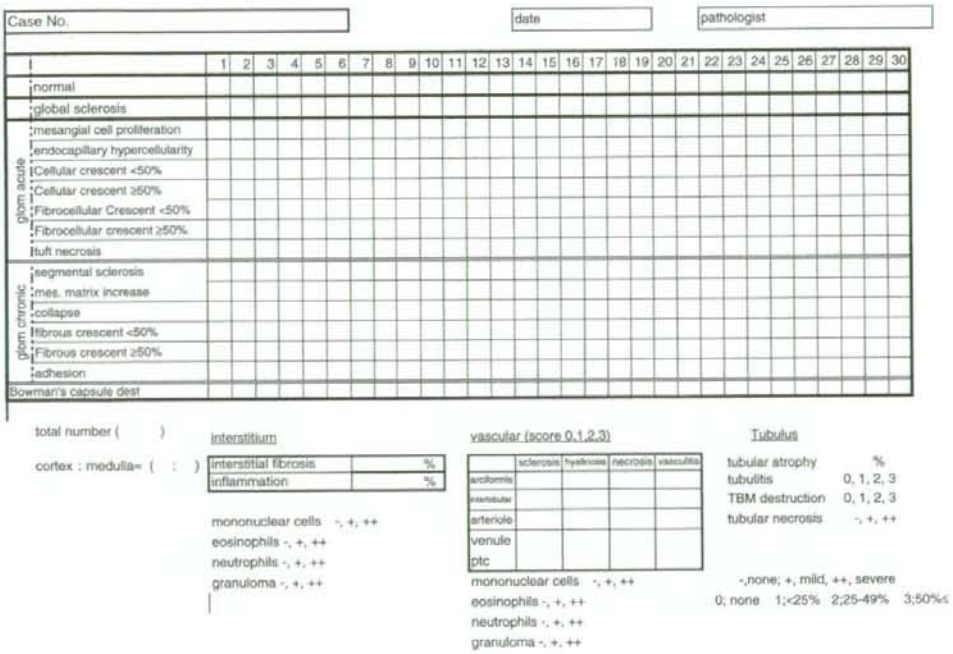

destruction of the TBM as well as the basement membrane of Bowman's capsule, the presence of granulomatous lesion in the arteries as well as the interstium, and vasculitis, including endarteritis. On the other hand, extraglomerular infiltrate, double contour of GBM and mesangial matrix increase from the EUVAS system as well as mesangiolysis, mesangial reticulation, mesangial expansion, and mesangial interposition from the Shigematsu scoring system were not adapted in order to maintain reproducibility. Extracapillary lesions, such as exudates into the urinary space, rupture of GBM, extracapillary inflammatory cells, parietal epithelial proliferation, pseudotubularization, and ingrowth interstitium from the Shigematsu scoring system, were not adopted, but were substituted by the term "tuft necrosis" or "crescent" (cellular, fibrocellular, and fibrous) in the present scoring system.

The extent of tubulointerstitial lesions, including interstitial inflammation and interstitial fibrosis with tubular atrophy, is assessed dichotomously or trichotomously in the EUVAS scoring system. The present system evaluates extended tubulointerstitial lesions more precisely. It is scored as the percentage involvement rounded to the closest 10% (i.e., <5% = 0%). Semiquantitative criteria for interstitial inflammation is evaluated according to the extent of inflammatory cells in the cortex 0 = no or trivial interstitial inflammation (<10% of unscarred parenchyma), 1 = 10–25% of parenchyma inflamed, 2 = 26–50% of parenchyma inflamed, 3 = more than 50% of parenchyma inflamed. The grade of intraepithelial infiltrate (tubulitis), destruction of TBM, and acute tubular necrosis is expressed as the extent of tubulitis (0 = <10% of unscarred parenchyma, 1 = 10–25% of parenchyma inflamed, 2 = 26–50% of parenchyma inflamed, 3 = more than 50% of parenchyma inflamed). Semiquantitative criteria for interstitial fibrosis with tubular atrophy are evaluated according to the extent of interstitial fibrosis with tubular atrophy in the cortex: 0 = no or trivial interstitial fibrosis (<5% of unscarred parenchyma), 1 = 6–25% of interstitial fibrosis, 2 = 26–50% of interstitial fibrosis, 3 = more than 50% of interstitial fibrosis. Cell types of infiltrates (− = cell type is not present; + = cell type is present; ++ = cell type is predominantly present) for neutrophils, mononuclear cells, eosinophils, and granuloma were evaluated.

Vascular lesions are evaluated on arteries and arterioles dichotomously or trichotomously in the EUVAS scoring system. The present system evaluates vascular lesions more precisely. Arterial lesions are scored based on the most severe lesions, and arcuate artery, interlobular artery, arteriole, venule and peritubular capillary are evaluated with reference to sclerosis, necrosis, vasculitis (endarteritis), and thrombosis. The grade of intimal thickening (fibrosis) is shown (−, 1 < 25%; +, 26–50%; ++, >50% thickness of intima/thickness of total vascular wall). In addition, arteriolar hyaline is also noted as present or absent. Cell types of infiltrates (− = cell type is not present; + = cell type is present; ++ = cell type is predominantly present) for neutrophils, mononuclear cells, eosinophils, and granuloma were evaluated.

Discussion

(1) Why is our proposal based on the EUVAS scoring system and how did we develop this system?

The present study outlined the histologic parameters of renal ANCA-related vasculitis in an effort to standardize the diagnosis of the disease in Japan. In order to create a new scoring system, we reviewed both Shigematsu's scoring system and the EUVAS scoring system. Shigematsu's grading and staging system consists of the average score of various glomerular and tubulointerstitial lesions and is therefore not suitable to select each glomerular and tubulointerstitial parameter for distribution as a prognostic marker. Moreover, this system does not take vascular lesions into account. The EUVAS scoring system systematically reviews the critical histological parameters. Consequently, the proposed scoring system was principally based on the EUVAS scoring system, and basic pathological parameters were selected and added to consider renal involvement in Japanese ANCA-related vasculitis (Table 1). This system uses two different types of evaluation. First, many glomerular lesions were scored quantitatively as a percentage of the total number of glomeruli. Second, other pathological parameters (e.g., some glomerular parameters as well as interstitial and vascular data) were scored dichotomously or trichotomously according to a present/absent or −, +, and ++ scale. According to an international survey study, data on inter- and intra-observer agreement gave more favorable results for the analysis of quantitative data than for dichotomous scoring systems. This result indicates that when the observers were obligated to review the biopsies more comprehensively, the inter- and intra-observer agreement was clearer than when a simple decision, such as in a dichotomous scoring system, was required [7]. Therefore, the present scoring system requires quantitative evaluation not only of glomerular lesions, but also tubulointerstitial and vascular lesions.

(2) What can the quantitative evaluation of glomerular, tubulointerstitial, and vascular lesions bring?

Semiquantitative evaluation of tubulointerstitial and vascular lesions was adopted in the present scoring system, as well as facilitated statistical evidence about the correlation between histological and clinical parameters. The EUVAS histological scoring system also showed the successful study of histopathological analysis of renal biopsies and evaluated its correlation with renal functioning. The predictive value of clinical, serological, and histological parameters for the renal outcome were analyzed by multivariate analysis, resulting in an index that is valid for clinical use. Specifically, the formula for the estimation of renal function at 18 months is as follows: GFR (glomerular filtration rate) 18 (ml/min) = 17 + 0.71 × GFR0 (ml/min) + 0.34 × fibrinoid necrosis (%) + 0.33 × segmental crescents (%) ($r^2 = 0.60$; standard deviation = 19 ml/min) [12].

(3) Why should the vascular lesion be evaluated respecting the level of artery?

Vascular lesions in each arcuate artery, interlobular artery, and arteriole need to be evaluated in the present scoring system, because a differently affected level of renal

vasculature in ANCA-related vasculitis between Europe and Japan has been noticed. Histological evidence of small-vessel arteritis in ANCA-related vasculitis is rare (about 15% of cases) even with a lower prevalence of medium-vessel arteritis in Europe. In the recent EUVAS MEPEX (randomized trial of adjunctive therapy for severe glomerulonephritis in ANCA-related systemic vasculitis-intravenous administration of methylprednisolone versus plasma exchange) study of 100 renal biopsies, the frequency of small-vessel arteritis was 11%, and the frequency of medium-sized arteritis was 4% [13]. Preliminary data from 72 cases of MPO-ANCA-related vasculitis from a Japanese study group detected 21 out of 72 cases (29.1%), including arteriolar vasculitis (13 out of 72 cases, 18.1%), interlobular arteritis (8 out of 72 cases, 11.1%), and arcuate arteritis in 1 case. Although the definition of the term "medium-sized artery" in the kidney is still controversial, it suggests possible immunological and morphological differences between Japanese and European populations as well as potential differences in genetic and environmental factors and/or pathogenetic morphogenetic mechanisms. PN mainly affects medium-sized vessels and can be differentiated from WG, MPA, and CSS by the absence of glomerular lesions according to CHCC definitions [2]. However, there have been a few reports of large vessel involvement in ANCA-related vasculitides in Japan, as shown in Fig. 12, and in North America and Europe [22].

(4) Why should the presence of granulomatous lesion in the artery and in the interstitium be evaluated?

The presence of granulomatous lesions in the arteries as well as in the interstium was also evaluated in the present system. The extent of destruction of the TBM as well as of the basement membrane of Bowman's capsule is also assessed, because this destruction induces a granulomatous lesion, and the grade of tubulitis and TBM destruction was correlated with the titer of C-reactive protein (CRP) (our preliminary data; abstract in the International Symposium of Vasculitides, September 29, 2007, Tokyo). According to CHCC definitions, granulomatous inflammation of an artery or perivascular interstitial area is found in WG, whereas pauci-immune necrotizing glomerulonephritis is common to both MPA and WG [2]. Therefore, the principal difference between these two entities may be the presence of granulomatous inflammation in the latter disease; however, according to our experience in Japan, this histological criterion does not help to discriminate WG from MPA. Indeed, in almost all cases, patients with positive MPO-ANCA showed a renal lesion, which is essentially indistinguishable from patients with classical WG showing an extrarenal granulomatous lesion in the upper respiratory tract or in the lung. In terms of the differential diagnosis of WG versus MPA, a consensus stepwise algorithm has been developed using criteria from the American College of Rheumatology (ACR) and CHCC. It can successfully categorize ANCA-positive patients into a single classification [23]. Whether the presence of a granulomatous lesion is a hallmark of WG remains to be solved in the future. CSS, allergic granulomatosis and angiitis, is often found in the context of vascular and extravascular granulomatosis containing a large number of eosinophils. Clinically, bronchial asthma and eosinophilia are found. Renal involvement is present in 25% of all cases, reflecting the relatively benign course when compared with MPA [24]. The presence of these criteria, including eosinophil-rich and granulomatous inflammation involving the respiratory tract, necrotizing and granulomatous arteritis affecting small to medium-sized vessels, asthma, and eosinophilia, yields a sensitivity of 85% and a specificity of 99.7% for the diagnosis of Churg-Strauss arteritis [25]. This is also a reason to evaluate the presence of granulomatous lesion in the arteries as well as in the interstium.

(5) Is there any difference between MPO-ANCA- and PR3-ANCA (ANCA directed against pronase 3 as determined by ELISA)-related vasculitis concerning the histology and the prevalence in Asia and Europe?

Knowledge of the differences in renal histopathology between MPO-ANCA- and PR3-ANCA-related vasculitis or MPA and WG is relatively limited, although distinct histologic differences may help to establish a more definite diagnosis and may give insights into the pathogenesis of ANCA-related vasculitis. One study of 173 renal biopsies reported that the characteristics of chronic injury were more prevalent in biopsies from patients with MPA than with WG, which suggests that the pathogenesis and/or course of these diseases may be distinct [11]. Franssen et al. reported that patients with PR3-ANCA positivity had more fibrinoid necrosis and a higher activity index than those with MPO-ANCA positivity and that patients with MPO-ANCA had more glomerulosclerosis and a higher chronicity index [26]. By contrast, other studies have reported contradictory results or no differences between these groups [27, 28]. MPO-ANCA-related vasculitis is prominent in Japan and China, whereas PR3-ANCA is common in Europe. Patients with MPO-ANCA-positive WG are often found in the Chinese population and have been analyzed with regard to the histological differences between MPO- and PR3 ANCA-positive WG [29]. Two nationwide Japanese surveys demonstrated that the prevalence of patients with WG is very low compared with that of patients with microscopic polyangiitis (MPA) [30] and/or renal limited vasculitis (RLV) [31]. In Japan, the annual prevalence (i.e., the estimated number of patients treated in 1997) of WG is only 2.3 per million, whereas that of MPA and/or RLV is approximately 13.8 per million [30, 31].

Furthermore, MPO-ANCA was identified in 79–93% of patients with MPA and/or RLV in Japan, whereas reports from Europe described a percentage of 44–69% [11, 32–35]. Fujimoto et al. [36] reported that the estimated annual incidence of primary renal vasculitis in Miyazaki Prefecture was 14.8 (95% CI 10.8–18.9) and 44.8 (95% CI 33.2–56.3) per million adults (>15 year old) and seniors (>65 year old), respectively. Another study of rapidly progressive glomerulonephritis in Japan characterized subtypes as p-ANCA-related glomerulonephritis (67.3%), c-ANCA-related glomerulonephritis (4.7%), ANCA-negative pauci-immune type glomerulonephritis (6.4%), anti-GBM glomerulonephritis (8.8%), and lupus nephritis (8.2%) [15].

(6) Problems remain to be solved in the future

A disease condition presenting with only pauci-immune focal necrotizing glomerulonephritis, crescentic glomerulonephritis, or arteritis in the absence of other organ system involvement is generally classified as "renal-limited" vasculitis (RLV). In Japan, laboratory testing for ANCA is supported financially by national insurance. Thus, many more patients are being diagnosed and treated in an early stage of disease, resulting in higher rates of remission before the full clinical course becomes apparent. Later clinical manifestations may follow, suggesting the onset of vasculitis in other systemic organs. It has not yet been determined whether combined systemic vasculitis or late onset of systemic vasculitis occurs more frequently when RLV patients show not only necrotizing glomerulonephritis, but also medium-sized or small arteritis. These problems remain to be solved in the future.

In Japan, the histology-based therapeutic choice for ANCA-related glomerulonephritis is still uncertain. Sakai et al. reported the impact of a histologic scoring system, including the distribution and stage of crescents, and grade of tubulointerstitial lesions for an outcome prediction, but it is insufficient to guide the choice of therapy [15]. Thus, a future study to characterize optimal treatment regimens based on histological distinctions of ANCA-related vasculitis would be of benefit. This classification will also be applied for anti-GBM nephritis (nephritis in Goodpasture syndrome) and idiopathic crescentic glomerulonephritis.

Acknowledgments The authors are grateful for the tremendous support of Kazuo Suzuki (Chiba University Graduate School of Medicine, Inflammation Program, Department of Immunology), Satoko Kawashima (First Department of Internal Medicine, Kyorin University School of Medicine), Hiroaki Komori (Department of Pathogenomics, Ehime University Graduate School of Medicine), Mitsuyo Itabashi (Department of Medicine, Kidney Center, Tokyo Women's Medical University), Noriaki Sada (Departments of Medicine and Clinical Science Okayama University Graduate School of Medicine), Tomoyoshi Kimura (Department of Nephrology, Sendai Shakaihoken Hospital), Kengo Furuichi (Division of Blood Purification, Kanazawa University Hospital, Department of Gastroenterology and Nephrology), Yukio Yuzawa (Department of Nephrology, Nagoya University Graduate School of Medicine), and Akira Horikoshi (Division of Nephrology, Department of Internal Medicine, Juntendo University School of Medicine) and Hiroyuki Kanno, Department of Pathology, Iwate Medical University). This study was supported by a grant from the Japan Health Science Foundation on "Research on Health Sciences focusing on Drug Innovation, International Collaborative Research (SH 44410)" (Chairperson Hiroshi Hashimoto), Renal Pathology Committee of JMAAV (Japanese study group for MPO-ANCA-related vasculitis), the joint committee of "Progressive Renal Diseases" (Chairperson: Yasuhiko Tomino) and "Intractable Vasculitis Syndromes" (Chairperson: Shoichi Ozaki) of the Ministry of Health, Labor and Welfare of Japan.

References

1. Jeannette JC, Thomas DB. Pauci-immune and antineutrophil cytoplasmic autoantibody-mediated crescentic glomerulonephritis and vasculitis. In: Jeannette JC, Olson JL, Schwartz MM, Silva FG, editors. Heptinstall's pathology of the kidney. 6th ed. Philadelphia: Lippincott Williams & Wilkins; 2007. pp. 645–700.
2. Jeannette JC, Falk RJ, Andrassy K, Bacon PA, Churg J, Gross WL, et al. Nomenclature of systemic vasculitides: proposal of an international consensus committee. Arthritis Rheum. 1994;37:187–92.
3. Guillevin L, Durand-Gasselin B, Cevallos R, Gayraud M, Lhote F, Callard P, et al. Microscopic polyangiitis: clinical and laboratory findings in 85 patients. Arthritis Rheum. 1999;42:421–30.
4. Levy J. New aspects in the management of ANCA-positive vasculitis. Nephrol Dial Transplant. 2001;16:1314–7.
5. Jayne D, Rasmussen N, Andrassy K, Bacon P, Tervaert JW, Dadoniene J, et al. A randomized trial of maintenance therapy for vasculitis associated with antineutrophil cytoplasmic autoantibodies. N Engl J Med. 2003;349:36–44.
6. Jayne DR, Gaskin G, Rasmussen N, Abramowicz D, Ferrario F, Guillevin L, et al. Randomized trial of plasma exchange or high-dosage methylprednisolone as adjunctive therapy for severe renal vasculitis. J Am Soc Nephrol. 2007;18:2180–8.
7. Bajema IM, Hagen EC, Hansen BE, Hermans J, Noel LH, Waldherr R, et al. The renal histopathology in systemic vasculitis: an international survey study of inter- and intra-observer agreement. Nephrol Dial Transplant. 1996;11:1989–95.
8. Bajema IM, Hagen EC, Hermans J, Noel LH, Waldherr R, Ferrario F, et al. Kidney biopsy as a predictor for renal outcome in ANCA-related necrotizing glomerulonephritis. Kidney Int. 1999;56:1751–8.
9. Hauer HA, Bajema IM, Van Houwelingen HC, Ferrario F, Noel LH, Waldherr R, et al. Determinants of outcome in ANCA-related glomerulonephritis: a prospective clinico-histopathological analysis of 96 patients. Kidney Int. 2002;62:1732–42.
10. Hauer HA, Bajema IM, Hagen EC, Noel LH, Ferrario F, Waldherr R, et al. Long-term renal injury in ANCA-related vasculitis: an analysis of 31 patients with follow-up biopsies. Nephrol Dial Transplant. 2002;17:587–96.
11. Hauer HA, Bajema IM, van Houwelingen HC, Ferrario F, Noel LH, Waldherr R, et al. Renal histology in ANCA-related vasculitis: differences between diagnostic and serologic subgroups. Kidney Int. 2002;61:80–9.
12. Vergunst CE, van Gurp E, Hagen EC, van Houwelingen HC, Hauer HA, Noel LH, et al. An index for renal outcome in ANCA-related glomerulonephritis. Am J Kidney Dis. 2003;41:532–8.
13. de Lind van Wijngaarden RA, Hauer HA, Wolterbeek R, Jayne DR, Gaskin G, Rasmussen N, et al. Clinical and histologic determinants of renal outcome in ANCA-related vasculitis: a

prospective analysis of 100 patients with severe renal involvement. J Am Soc Nephrol. 2006;17:2264–74.
14. de Lind van Wijngaarden RA, Hauer HA, Wolterbeek R, Jayne DR, Gaskin G, Rasmussen N, et al. Chances of renal recovery for dialysis-dependent ANCA-related glomerulonephritis. Am Soc Nephrol. 2007;18:2189–97.
15. Sakai K, Kurokawa K, Koyama A, Arimura Y, Kida H, Shigematsu S, et al. Committee for the guidelines on diagnosis and therapy of rapidly progressive glomerulonephritis: the guidelines for the management of rapidly progressive glomerulonephritis [in Japanese]. Jpn J Nephrol. 2002;44:55–83.
16. Shigematsu H, Yamaguchi N, Koyama A. Glomerulointerstitial events in rapidly progressive nephritic syndrome, with special reference to histologic grade and stage on the renal lesions. Clin Exp Nephrol. 1998;2:330–8.
17. Weening JJ, D'Agati VD, Schwartz MM, Seshan SV, Alpers CE, Appel GB, et al. The classification of glomerulonephritis in systemic lupus erythematosus revisited. Kidney Int. 2004;65:521–30.
18. Word Health Organization. Section 1. Classification of glomerular diseases. Glossary of terms. In: Churg J, Bernstein J, Glassock RJ, editors. Renal disease classification and atlas of glomerular diseases. 2nd ed. Tokyo: IGAKU-SHOIN; 1995. pp. 3–26.
19. Racusen LC, Solez K, Colvin RB, Bonsib SM, Castro MC, Cavallo T, et al. The Banff 97 working classification of renal allograft pathology. Kidney Int. 1999;55:713–23.
20. Word Health Organization. Section 1. Introduction and classification. In: Seshan S, D'agati V, Appel G, Churg J, editors. Renal disease classification and atlas of tubulointerstitial and vascular diseases. 2nd ed. New York: William Wilkins; 1999. p. 3–12.
21. Arkin A. A clinical and pathological study of periarteritis nodosa. A report of 5 cases, one histologically healed. Am J Pathol. 1936;6:401–27.
22. Chirinos JA, Tamariz LJ, Lopes G, Del Carpio F, Zhang X, Milikowski C, et al. Large vessel involvement in ANCA-related vasculitides: report of a case and review of the literature. Clin Rheumatol. 2004;23:152–9.
23. Watts R, Lane S, Hanslik T, Hauser T, Hellmich B, Koldingsnes W, et al. Development and validation of a consensus methodology for the classification of the ANCA-related vasculitides and polyarteritis nodosa for epidemiological studies. Ann Rheum Dis. 2007;66:222–7.
24. Sinico RA, Di Toma L, Maggiore U, Tosoni C, Bottero P, Sabadini E, et al Renal involvement in Churg-Strauss syndrome. Am J Kidney Dis. 2006;47:770–9.
25. Masi AT, Hunder GG, Lie JT, Michel BA, Bloch DA, Arend WP, et al. The American College of Rheumatology 1990 criteria for the classification of Churg-Strauss syndrome (allergic granulomatosis and angiitis). Arthritis Rheum. 1990;33:1094–100.
26. Franssen CF, Stegeman CA, Kallenberg CG, Gans ROB, de Jong PE, Hoorntje SJ, et al. Antiproteinase 3- and antimyeloperoxidase-associated vasculitis. Kidney Int. 2000;57:2195–206.
27. Jennette JC, Wilkman AS, Falk RJ. Anti-neutrophil cytoplasmic autoantibody-associated glomerulonephritis and vasculitis. Am J Pathol. 1989;135:921–30.
28. Fienberg R, Mark EJ, Goodman M, McCluskey RT, Niles JL. Correlation of antineutrophil cytoplasmic antibodies with the extrarenal histopathology of Wegener's (pathergic) granulomatosis and related forms of vasculitis. Hum Pathol. 1993;24:160–8.
29. Chen M, Wang F, Yu S-X, Zou W-Z, Zhang Y, Zhao M-H, et al. Renal histology in Chinese patients with anti-myeloperoxidase autoantibody-positive Wegener's granulomatosis. Nephrol Dial Transplant. 2007;22:139–45.
30. Matsumoto Y, Inoba Y, Nakayama T, Tamakoshi A, Ohno Y, Kobayashi S, et al. Nationwide epidemiological survey of refractory vasculitis (anti-neutrophil cytoplasmic antibody (ANCA)-associated vasculitis, anti-phospholipid syndrome and temporal arteritis) in Japan. Annual Report of the Research Committee on Intractable Vasculitides, the Ministry of Health and Welfare of Japan [in Japanese], Tokyo; 1998. p. 15–23.
31. Lane SE, Scott DG, Heaton A, Watts RA. Primary renal vasculitis in Norfolk: Increasing incidence or increasing recognition? Nephrol Dial Transplant. 2000;15:23–7.
32. Gonzalez-Gay MA, Garcia-Porrua C, Guerrero J, Rodriguez-Ledo P, Llorca J. The epidemiology of the systemic vasculitides in northwest Spain: implications of the chapel hill consensus conference definitions. Arthritis Rheum. 2003;49:388–93.
33. Tidman M, Olander R, Svalander C, Danielsson D. Patients hospitalized because of small vessel vasculitides with renal involvement in the period 1975–1995: organ involvement, ANCA patterns, seasonal attack rates and fluctuation of annual frequencies. J Intern Med 1998;244:133–41.
34. Booth AD, Almond MK, Burns A, Ellis P, Gaskin G, Neild GH, Plaisance M, Pusey CD, Jayne DRW. Outcome of ANCA-related renal vasculitis: a 5-year retrospective study. Am J Kidney Dis. 2003;41:776–84.
35. El-Reshaid K, Kapoor MM, El-Reshaid W, Madda JP, Varro J. The spectrum of renal disease associated with microscopic polyangiitis and classic polyarteritis nodosa in Kuwait. Nephrol Dial Transplant. 1997;12:1874–82.
36. Fujimoto S, Uezono S, Hisanaga S, Fukudome K, Kobayashi S, Suzuki K, et al. Incidence of ANCA-related primary renal vasculitis in the Miyazaki Prefecture: the first population-based, retrospective, epidemiologic survey in Japan. Clin J Am Soc Nephrol. 2006;1:1016–22.

Circ J 2008; **72:** 813–819

Alteration of IL-17 Related Protein Expressions in Experimental Autoimmune Myocarditis and Inhibition of IL-17 by IL-10-Ig Fusion Gene Transfer

He Chang, MD; Haruo Hanawa, MD; Tsuyoshi Yoshida, MD; Manabu Hayashi, MD; Hui Liu, MD; Limin Ding, MD; Keita Otaki, MD; Kazuhisa Hao, MD; Kaori Yoshida, BS; Kiminori Kato, MD; Ken Toba, MD; Makoto Kodama, MD; Hiroki Maruyama, MD*; Junichi Miyazaki, MD**; Yoshifusa Aizawa, MD

Background T-helper (Th)1/Th2 cytokine balance plays an important role in the pathogenesis of myocarditis. Recently, some studies indicate that interleukin (IL)-17, known as a T cell (Th17)-derived proinflammatory cytokine, is the major mediator of tissue inflammation in inflammatory and autoimmune diseases. Experimental autoimmune myocarditis (EAM) is a T cell-mediated autoimmune disease; however, the pathogenic role of IL-17 in the development of rat EAM remains largely unknown.

Methods and Results In the present study, alterations of IL-17-related protein expressions were investigated and then the effect of hydrodynamic-based delivery of plasmid DNA encoding the IL-10-Ig gene on rat EAM and the effect of IL-10-Ig on IL-17 was evaluated. The results showed that IL-17 was expressed more highly than IFN-γ expressed by Th1 cells in $\alpha\beta$T cells and the peaks of IL-17 related protein expression in the heart were the early phase of EAM. Moreover, we observed that IL-10-Ig gene therapy was effective in controlling EAM and that IL-10-Ig significantly suppressed the expression of IL-17 as well as other proinflammatory cytokines, IL-1β and TNF-α, in IL-1-stimulated splenocytes cultured from EAM rats.

Conclusions IL-17 is highly produced by $\alpha\beta$T cells in the early phase of EAM hearts and IL-17 inhibition might be a possible mechanism of the amelioration of EAM by IL-10-Ig treatment. These data suggest that IL-17 produced by Th17 plays an important role in the pathogenesis of rat EAM. (*Circ J* 2008; **72:** 813–819)

Key Words: Cardiomyopathy; Gene therapy; Interleukin-17; Th17; Th1/Th2 balance

Rat experimental autoimmune myocarditis (EAM) induced by immunization with cardiac myosin is a T cell-mediated autoimmune disease transferred by spleen cells from EAM rats[1] and most infiltrating T cells are CD4+ T cells that express $\alpha\beta$T cell antigen receptors.[2,3] CD4+ T-helper (Th) cells are traditionally thought to differentiate into interleukin (IL)-2- and IFNγ-producing Th1 and IL-4-, IL-10- and IL-13-producing Th2 cell subsets.[4] It has been assumed that Th1/Th2 cytokine balance is important in myocarditis.[5–7] Recently, however, Th17 has been reported to play an important role for various models of immune-mediated tissue injury, including organ-specific autoimmunity.[8,9] Th17 produces IL-17 and it is a proinflammatory cytokine that activates T cells and other immune cells to produce a variety of cytokines, chemokines and cell adhesion molecules.[10] IL-17 cannot be categorized as either Th1 or Th2 cytokine by cytometric single-cell analysis of Th cell cytokine production.[11] Th17 is a new CD4+ helper T cell subset characterized by producing IL-17.[12] Th17 cells are activated by IL-23, which is thought to be produced by activated macrophages and dendritic cells,[8] via a receptor complex composed of IL-12 receptor β1 (IL-12Rβ1) and IL-23 receptor (IL-23R).[13] IL-17 has been suggested to be involved in the development of rheumatoid arthritis[14] and experimental autoimmune encephalomyelitis (EAE).[10] Recently, it has been reported that mice lacking T-bet, a T-box transcription factor required for Th1 cell differentiation, develop severe autoimmune myocarditis by immunization with myosin heavy chain peptide and anti-IL-17 antibody or neutralization of IL-17 by active vaccination therapy, which markedly reduced mice EAM severity.[15,16] However, in rat EAM hearts, the time-course of expression of IL-17 related proteins and their producing- or targeting-cells has not been determined.

Th1 T cells producing IL-2 and IFN-γ infiltrate the heart in the early phase of EAM and are estimated to play an important role in triggering EAM. In contrast, Th2 cytokines, IL-4, IL-10 and IL-13 and so on, are thought to play an important role in the control of T-cell-mediated autoimmunity. We have previously reported that IL-10 and IL-13 ameliorated EAM[17,18] and IL-10 expression increased later than Th1 cytokine in the EAM heart.[19] Recent studies have

(Received July 30, 2007; revised manuscript received November 24, 2007; accepted December 11, 2007)

*Divisions of Cardiology, *Clinical Nephrology and Rheumatology, Niigata University Graduate School of Medical and Dental Sciences, Niigata and **Division of Stem Cell Regulation Research, Osaka University Medical School, Suita, Japan*

Mailing address: Haruo Hanawa, MD, Division of Cardiology, Niigata University Graduate School of Medical and Dental Sciences, 1-757 Asahimachi-dori, Niigata 951-8120, Japan. E-mail: hanawa@med.niigata-u.ac.jp

shown that both IFN-γ (Th1 cytokine) and IL-4 (Th2 cytokine) negatively regulated the T helper cell production of IL-17 in the effector phase[9,20]. IL-10 is one of the Th2 cytokines, however, the relationship between IL-10 and IL-17 is still unknown in autoimmune disease models. IL-10 in EAM hearts was mainly detected in non-cardiomyocytic non-inflammatory (NCNI) cells (mainly fibroblasts, smooth muscle cells, and endothelial cells)[21] and IL-10-targeting cells, which expressed both IL-10R1 and IL-10R2, were mainly T cells expressing $\alpha\beta$T cell antigen receptors ($\alpha\beta$T cells) and CD11b$^+$ cells (macrophages/dendritic cells/granulocytes) in EAM hearts[21,22]. Several studies have demonstrated the therapeutic effect of IL-10 in various autoimmune/inflammatory diseases. In myocarditis, IL-10 inhibited the secretion of proinflammatory cytokines such as TNF-α, IFN-γ, iNOS, IL-2 and IL-12 and displayed major effects on immune cells[23,24].

In this study, we examined the time-course and expression cells of IL-17, IL-17R, IL-23 and IL-23R in EAM hearts, the effect of hydrodynamic-based delivery of the IL-10-Ig fusion gene in rat EAM, and the effect of IL-10 on the expression of IL-17 and proinflammatory cytokines.

Methods

Animals

Eight-week-old male Lewis rats were purchased from Charles River Laboratories and were maintained at our animal facilities. Throughout the studies, all of the animals were treated in accordance with the guidelines for animal experiments as laid out by our institute (Animal Resources Branch of Niigata University, Niigata, Japan).

Induction of EAM

Whole cardiac myosin was prepared from the ventricular muscle of porcine hearts as previously described[25]. It was dissolved in a solution of 0.3 mol/L KCl at a concentration of 10 mg/ml. To produce EAM, on day 0, each rat was immunized with 0.2 ml of an emulsion containing cardiac myosin with an equal volume of complete Freund's adjuvant (CFA) by a single s.c. injection in both footpads. Rats were immunized with CFA alone as the control group.

Quantification of IL-17, IL-17R, IL-23, IL-23R, IL-10 and IFN-γ mRNA in EAM Hearts

To examine the time-course of IL-17, IL-17R, IL-23, IL-23R, IL-10 and IFN-γ expression in EAM, total RNA was isolated from EAM hearts on day 0 (n=3), 6 (n=4), 9 (n=3), 12 (n=3), 15 (n=5) and 18 (n=4) using TRIzol (Invitrogen Life Technologies, Tokyo, Japan), and cDNA was synthesized from 2-5μg of total RNA with random primers and murine Moloney leukemia virus reverse transcriptase. To create the plasmids used for the standard, IL-17, IL-17R, IL-23, IL-23R, IL-10 and IFN-γ mRNA were amplified from an EAM heart-derived cDNA library using the primer pairs (IL-17, sense primer 5'-tactcatccctcaaagttcagtgt-3', antisense primer 5'-ctcttgctggatgagaacagaat-3'; IL-17R, sense primer 5'-cacaagtccaagaccatcttagtg-3', antisense primer 5'-agacttgctcagagtgaatgtgac-3'; IL-23, sense primer 5'-aagagaagaagggaagaagagac-3', antisense primer 5'-gatcttggaacggagaagagaac-3'; IL-23R, sense primer 5'-aagtggctttatgaagatattccc-3', antisense primer 5'-atttgaaacctgggggtttgtatc-3') and primer pairs for IL-10 and IFN-γ[21]. PCR-amplified cDNA inserts were directly inserted into the pGEM-T easy vector, and recombinant plasmids were isolated following transformation into *Escherichia coli* (*E. coli*) JM109-competent cells using a MagExtractor plasmid kit (Toyobo, Osaka, Japan). Absolute copy numbers of their mRNA were also measured by quantitative real-time RT-PCR using a LightCycler instrument together with the same primers and SYBR Premix Ex Taq (Takara, Otsu, Japan). The absolute copy numbers of particular transcripts were calculated by LightCycler software using a standard curve approach[19].

RNA Extraction From Cells Separated From the EAM Heart

To evaluate IL-17, IL-23 and IFN-γ producing and targeting cells, the expression of IL-17, IL-17R, IL-23, IL-23R, IL-12Rβ1 and IFN-γ genes was examined in cardiomyocytes (n=5), $\alpha\beta$T cells (n=5), CD11b$^+$ cells (n=5), and NCNI cells (n=6) (mainly fibroblasts, smooth muscle cells, and endothelial cells) in the hearts of EAM rats on day 18 by quantitative real-time RT-PCR using the primer pairs described above and the primer pairs for IL-12Rβ1 (sense primer 5'-ggacttgagctgctacagggtttc-3', antisense primer 5'-tccagttgtacaggtactgcgata-3'). These cells were isolated after collagenase perfusion treatment for 20 min using Langendorff apparatus as reported previously[21]. Briefly, isolated cells were separated serially through 38μm and 20μm stainless steel sieves twice into cardiomyocytes and other cells respectively. Because almost all inflammatory cells in EAM are $\alpha\beta$T cells and CD11b$^+$ cells[2], the other cells were separated into $\alpha\beta$T cells, CD11b$^+$ cells and NCNI cells such as fibroblasts, smooth muscle cells or endothelial cells by anti-PE micro beads (Miltenyi Biotec, Bergisch Gladbach, Germany) and a MACS magnetic cell sorting system (Miltenyi Biotech) using appropriate monoclonal antibodies, namely PE-conjugated TCR$\alpha\beta$ (R73) and CD11b (OX-42) (Pharmingen, San Diego, CA, USA). Total RNA was isolated from each purified cell fraction of EAM hearts using TRIzol. cDNA synthesis and quantification of IL-17, IL-17R, IL-23, IL-23R, IL-12Rβ1 and IFN-α mRNA were executed as described above.

Construction of Plasmid DNA for Gene Transfer

We prepared the plasmid vector pCAGGS-Ig-glucagon (GLU)-tag containing SwaI and NotI restriction sites, the control plasmid, pCAGGS-rat signal peptide (SP)-Ig-GLU-tag, the SP region of the secretory leukocyte protease inhibitor, as previously described[26]. To construct the pCAGGS-rat IL-10-Ig-GLU-tag plasmid, rat IL-10 was amplified from EAM heart cDNA using the primers 5'-ttcATTTAAATgcctggctcagcactgctatgt-3' and 5'-gcatcGCGGCCGCattttttcattttgagtgtcacgta-3', followed by insertion into a pCAGGS-Ig-GLU-tag using SwaI and NotI sites. *E. coli* JM109-competent cells were then transformed, and recombinant plasmids were isolated using a Quantum Prep Plasmid Maxiprep kit (Bio-Rad, Hercules, CA, USA).

Hydrodynamic-Based Plasmid DNA Encoding IL-10-Ig Gene Injection

Twenty-four rats were divided into 3 groups (CFA group n=6, IL-10-Ig group n=10, SP-Ig group n=8). CFA group rats were immunized with CFA on day 0. IL-10-Ig and SP-Ig groups rats were immunized with cardiac myosin emulsified in CFA on day 0 and injected with 800μg of a pCAGGS-rat IL-10-Ig-GLU-tag or a pCAGGS-SP-Ig-GLU-tag mixed with the appropriate volume of Ringer's solution (receiving approximately 80 ml/kg of body weight) via the tail vein within 15 s on day 1, respectively[27]. We previously showed the

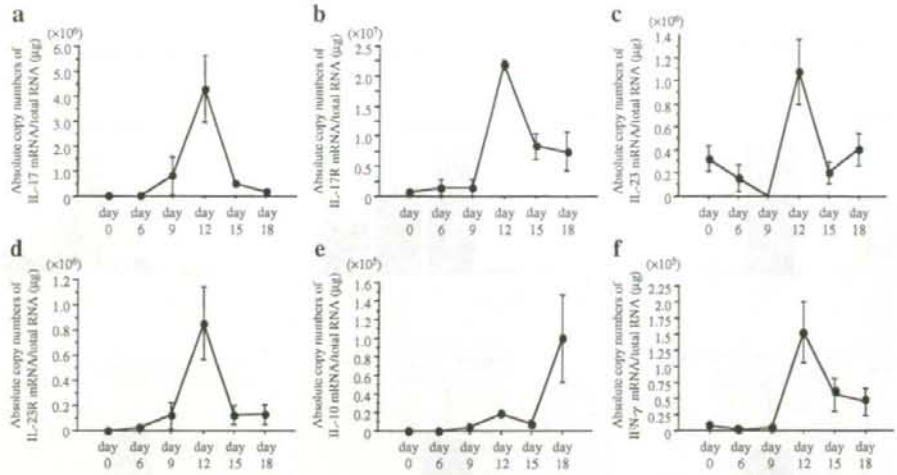

Fig 1. Time-course of interleukin (IL)-17 (a), IL-17 receptor (R) (b), IL-23 (c), IL-23R (d), IL-10 (e) and IFN-γ (f) mRNA expression in experimental autoimmune myocarditis hearts. Rats were immunized on day 0 (n=3) and killed on day 6 (n=4), day 9 (n=3), day 12 (n=3), day 15 (n=5) or day 18 (n=4). Absolute copy numbers of mRNA/total RNA were measured. Error bars represent SEM.

protection against EAM by the gene transfer of pCAGGS-mIL-10 by in vivo electroporation,[17] while in this study we used a hydrodynamic-based gene transfer of pCAGGS-rat IL-10-Ig because this method was thought to be more effective than in vivo electroporation and chimeras with immunoglobulin-facilitated elevated concentration levels.

Plasma Chimeric GLU-Tag Protein Measurement

To measure plasma concentrations of IL-10-Ig-GLU-tag proteins during the treatment course, blood samples were taken on days 2, 7, 12, and 17 after the hydrodynamics-based gene transfer on day 1. GLU concentrations were measured using a GLU RIA kit (Daiichi Radioisotope Laboratories, Tokyo, Japan). Chimeric protein concentrations were calculated using a GLU-tag.[28]

Evaluation of Histopathology

All rats were killed on day 17. The heart weight without atria and the body weight were measured, and the ratio of heart weight to body weight (g/g) was calculated. The hearts were cut into three 4μm-thick transverse sections for Azan-Mallory staining. The myocarditis areas were determined using specimens stained with Azan-Mallory by a color image analyzer (MacSCOPE, version 2.6; Mitani, Japan).

Expression of ANP mRNA in the Heart

In order to examine the effect of therapy, the amounts of ANP mRNA as a heart failure marker were measured.[29,30] RNA was extracted from the hearts of rats on day 17 and cDNA was synthesized as described above. ANP mRNA was measured by quantitative real-time RT-PCR using the primer pairs (sense primer 5'-atggatttcaagaacctgctagac-3', antisense primer 5'-gctccaatcctgtcaatcctac-3').[19] Cox6a2 mRNA as a control was measured using the primer pairs (sense primer 5'-cgcatccaaaggagaccac-3', antisense primer 5'-aaaggattgacgtggggatt-3'). The plasmids used for the standard were constructed as described above.

Preparation of Medium or Serum Containing IL-10-Ig for Spleen Cell Culture

For preparation of medium containing IL-10-Ig-GLU or Ig-GLU, Cos-7 cells (ATCC, Rockville, MD, USA) were cultured on 35 mm-well dishes in 2 ml of RPMI 1640 medium supplemented with 10% FCS for 24 h at 37°C in a humidified atmosphere (5% CO_2 and 95% air) and transfected with plasmids using FuGENE-6 (Roche Diagnostics, Indianapolis, IN, USA). Briefly, after reaching confluency, 3μl of FuGENE-6 was incubated in 97μl of serum-free RPMI 1640 medium for 5 min at room temperature and then 1μg of pCAGGS-IL-10-Ig-GLU or sp-Ig-GLU was added, mixed and incubated for 15 min at room temperature. The 100μl of the transfection reagent: DNA was added into each dish and incubated at 37°C in a humidified atmosphere (5% CO_2 and 95% air). After 24 h, the medium was changed and at 3 days after the medium was changed, the culture medium was collected and GLU concentrations were measured as described above. The concentration of IL-10-Ig-GLU or Ig-GLU in the medium was 5 nmol/L and we used the medium for spleen cell culture.

To prepare serum containing IL-10-Ig-GLU or Ig-GLU for spleen cells culture, normal rats were injected with 800μg of pCAGGS-rat IL-10-Ig-GLU-tag or pCAGGS-SP-Ig-GLU-tag mixed with the appropriate volume of Ringer's solution (receiving approximately 80 ml/kg of body weight) via the tail vein within 15 s, respectively, and after 24 h, the serum was collected. The concentation of IL-10-Ig-GLU or Ig-GLU in the serum was 5 nmol/L and we used the serum for spleen cell culture.

Spleen Cell Culture

Spleens were obtained from rats injected with EAM on day 14 and cultured to 6×10^6/ml on 35 mm-well dishes in 2 ml of RPMI 1640 medium supplemented with 10% FCS. Shortly after culture, spleen cells (n=5) were stimulated by adding rat IL-1α (final concentration of 1 ng/ml) (PeproTech, London, UK) and 100μl of IL-10 containing medium

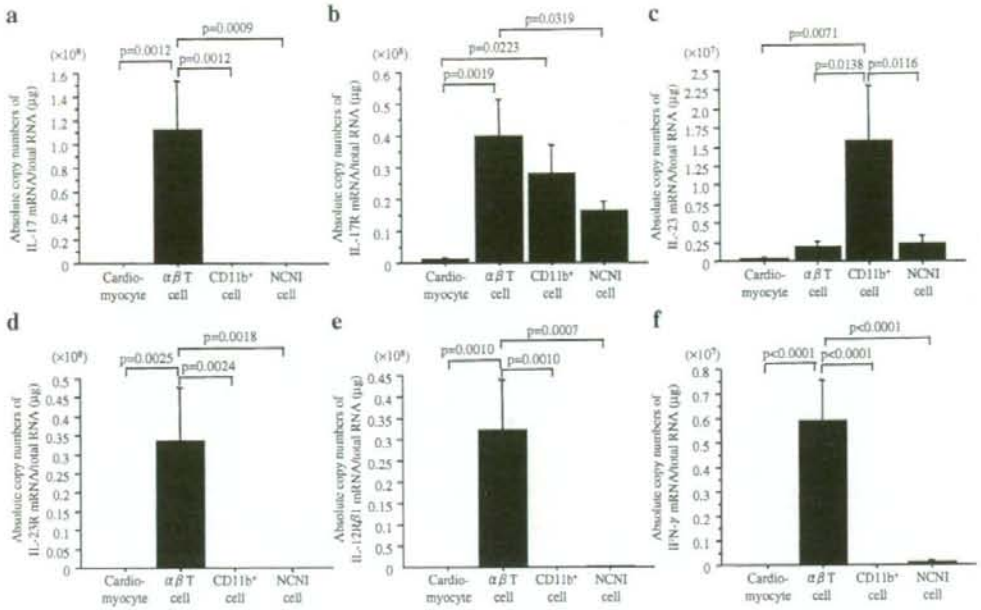

Fig 2. Absolute copy numbers of interleukin (IL)-17 (a), IL-17 receptor (R) (b), IL-23 (c), IL-23R (d), IL-12Rβ1 (e) and IFN-γ (f) mRNA. Each cell fraction (n=5 or 6) was separated and purified from experimental autoimmune myocarditis hearts on day 18. Non-cardiomyocytic non-inflammatory (NCNI) cells are mainly fibroblasts, smooth muscle cells and endothelial cells. Error bars represent SEM.

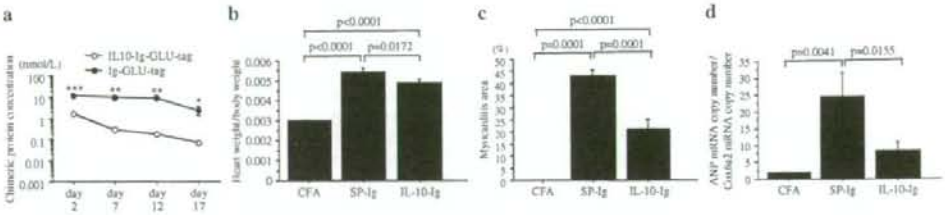

Fig 3. (a) Plasma interleukin (IL)-10-Ig-GLU-tag (n=10) and Ig-GLU-tag (n=8) protein levels. Chimeric protein concentrations were calculated by using the GLU-tag. ***p<0.001, **p<0.01, *p<0.05. (b) Heart weight to body weight ratio of complete Freund's adjuvant (CFA), IL-10-Ig-GLU-tag and SP-Ig-GLU-tag groups. The CFA group rats were only injected with CFA without cardiac myosin and were not at all affected with myocarditis. (c) Myocarditis area in experimental autoimmune myocarditis hearts of CFA, IL-10-Ig-GLU-tag and SP-Ig-GLU-tag groups by a color image analyzer. (d) The ratio of ANP mRNA to Cox6a2 in CFA, IL-10-Ig-GLU-tag and SP-Ig-GLU-tag groups. Error bars represent SEM.

obtained from Fugene-6 transfection with plasmid IL-10-Ig-GLU-tag or Ig-GLU-containing medium with plasmid SP-Ig-GLU-tag, or 100μl of IL-10-Ig-GLU-tag-containing serum obtained from an IL-10-Ig-treated normal rat or the same amount of an Ig-GLU-tag-containing serum from an SP-Ig-treated normal rat (the medium or serum IL-10-Ig-GLU or Ig-GLU final concentration was 0.25 nmol/L). After culturing for 24 h at 37°C, spleen cells were collected, total RNA was isolated, and cDNA was synthesized as described above. The absolute copy numbers of γ-actin, IL-17, IL-1β, TNF-α and IFN-γ mRNA were measured by quantitative real-time RT-PCR with previously reported primers[18,19]

Statistical Analysis

Statistical assessment was performed by using a non-paired Student's t-test or a one-way ANOVA and Bonferroni's multiple comparison test. Differences were considered significant at $p<0.05$. The heart weight to body weight ratio, myocarditis area, data obtained from quantitative RT-PCR and the concentrations of IL-10-Ig-GLU-tag and Ig-GLU-tag were expressed as the mean ± SEM.

Results

Time-Course of IL-17-Related Proteins mRNA in EAM Hearts

The onset of EAM is approximately 10 days after the injection of a cardiac myosin protein and the peak of inflammation is approximately on day 12 or day 15. mRNA of IL-17 and IL-23R in EAM hearts increased on day 9 and

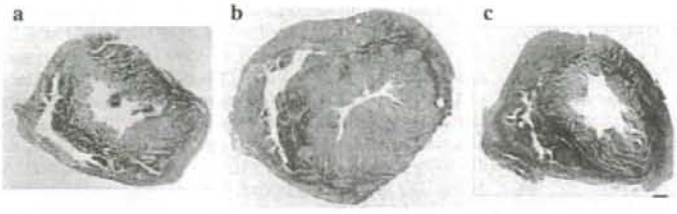

Fig 4. A histological examination of transverse sections in ventricles were stained with Azan-Mallory stain. (a) A transverse section of a heart in a complete Freund's adjuvant control group did not exhibit myocarditis. (b) Transverse sections of hearts in the SP-Ig-GLU-tag group. (c) Transverse sections of hearts in the IL-10-Ig-GLU-tag group. Bar represents 1 mm.

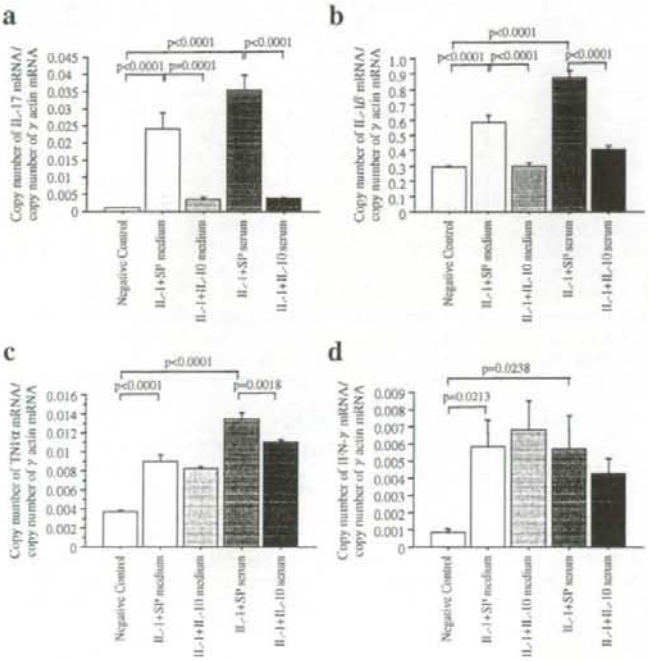

Fig 5. Copy numbers of interleukin (IL)-17 (a), IL-1β (b), TNF-α (c) and IFN-γ (d) mRNA per copy number of γ-actin mRNA in cultivated spleen cells (n=5) from experimental autoimmune myocarditis rats. Negative control, none of IL-1α, medium and serum; IL-1+SP medium, IL-1α (1 ng/ml) and 5% culture medium obtained from Cos-7 cells transfected with plasmid pCAGGS-SP-Ig-GLU-tag; IL-1+IL-10 medium, IL-1α (1 ng/ml) and 5% culture medium obtained from Cos-7 cells transfected with plasmid pCAGGS-IL-10-Ig-GLU-tag; IL-1+SP serum, IL-1α (1 ng/ml) and 5% serum obtained from a normal rat injected with pCAGGS-SP-Ig-GLU-tag; IL-1+IL-10 serum, IL-1α (1 ng/ml) and 5% serum obtained from a normal rat injected with pCAGGS-IL-10-Ig-GLU-tag. The final concentration of the IL-10-Ig protein or the SP-Ig protein in the culture dish was 0.25 nmol/L. Error bars represent SEM. Statistical assessment was performed by using a one-way ANOVA and Bonferroni's multiple comparison test (negative control vs IL-1+SP medium vs IL-1+IL-10 medium or a negative control vs IL-1+SP serum vs IL-1+IL-10 serum). Results are representative of 3 independent experiments.

mRNA of IL-17, IL-17R, IL-23, IL-23R and IFN-γ peaked on day 12. One of the most remarkable findings was a strong expression of IL-17. Absolute copy numbers of IL-17 mRNA were approximately 30-fold more than those of IFN-γ. In contrast, IL-10 mRNA was augmented on day 18 (Fig 1). The IL-10 expression in EAM hearts was later than for IL-17, IL-23, IL-17R, IL-23R and IFN-γ.

mRNA of IL-17-Related Proteins in Separated Cells From EAM Hearts

In EAM hearts on day 18, IL-17, IL-23R IL-12Rβ1 and IFN-γ were expressed mostly in $\alpha\beta$T cells fractions. Similarly to analysis of the time-course, one of the most remarkable findings was a strong expression of IL-17 in $\alpha\beta$T cells. Absolute copy numbers of IL-17 mRNA were approximately 20-fold more than those of IFN-γ. IL-17R was detected in $\alpha\beta$T cells, CD11b$^+$ and NCNI cell fractions. IL-23 was detected mostly in CD11b$^+$ cell fractions (Fig 2).

Time-Course of Plasma IL-10-Ig-GLU-Tag Protein Levels

During the course of treatment, plasma IL-10-Ig-GLU-tag protein levels in rats injected with pCAGGS-IL-10-Ig on day 1 increased to 1.73±0.25 nmol/L (mean±SEM) on day 2 and gradually decreased on days 7, 12, and 17 to 0.29±0.03, 0.18±0.03 and 0.07±0.02 nmol/L, respectively. Plasma Ig-GLU-tag protein levels in pCAGGS-SP-Ig control rats increased to 12.5±2.5 nmol/L on day 2 and decreased on days 7, 12 and 17, to 9.74±2.86, 8.99±2.52 and 2.36±1.06 nmol/L, respectively (Fig 3a). Although IL-10-Ig-GLU-tag serum levels were lower than that of control Ig-GLU-tag serum levels by hydrodynamic-based gene delivery, they were higher than the serum level found by in vivo electroporation gene transfer into a muscle[17] These results indicated that a continuous effective delivery of the IL-10-Ig-GLU-tag protein could be achieved in rats by hydrodynamic-based gene transfection.

Effect of In Vivo Treatment With Plasmid DNA Encoding the IL-10-Ig Gene

The heart weight to body weight ratio of the IL-10-Ig group was significantly less than that of the SP-Ig group (0.49±0.02 vs 0.54±0.02, p=0.0172) (mean±SEM) (Fig 3b). The inflammatory area of the ventricle transverse section in the IL-10-Ig group was significantly smaller than that in the

controls (21.3±3.2 vs 42.7±2.4, p=0.0001) (Fig 3c). Inflammation and fibrosis in the hearts of the SP-Ig-GLU-tag group was more severe than that of the IL-10-Ig group. The ratio of ANP mRNA to Cox6a2 as a heart failure marker in the IL-10-Ig group was significantly lower than that in controls (8.5±2.4 vs 24.6±7.3, p=0.0155) (Fig 3d). The hearts from immunized CFA control rats did not show inflammation (Fig 4).

mRNA Expression of IL-17 and Immunologic Molecules in Cultivated Spleen Cells After IL-10 Treatment

We examined the effect of IL-10 on the expression of IL-17 in cultivated spleen cells (n=5) from EAM rats on day 14. The concentration of the IL-10-Ig protein (final concentration of 0.25 nmol/L) used in the in vitro experiment is almost the same as that of serum in the early phase of EAM, when it was treated with a hydrodynamic-based IL-10-Ig gene transfer. The results showed that IL-17 was significantly enhanced by IL-1α and IL-10-Ig-containing medium and that serum significantly inhibited the gene expression of IL-17 in IL-1α-stimulated spleen cells from EAM rats (Fig 5). We also examined the effect of IL-10 on the expression of other proinflammatory cytokines such as IL-1β, TNF-α and IFN-γ in IL-1α-stimulated spleen cells from EAM rats, and the results showed that IL-10-Ig-containing medium or serum significantly inhibited the gene expressions of IL-1β and TNF-α, however, IFN-γ was not significantly inhibited by IL-10-Ig-containing medium or serum (Fig 5).

Discussion

IL-17 was expressed in the early phase of EAM. The time-course of the expression of IFN-γ was similar to that of IL-17 in EAM hearts. Because EAM is a T-cell-mediated disease[1] and most of the infiltrating T cells in EAM are $CD4^+$,[2] Th17 cells producing IL-17 might trigger or sustain inflammatory events in the heart. Until recently, we have suggested that Th1 cells producing IFN-γ or IL-2 played an important role as a trigger of EAM; however, in this study, our results indicate that absolute copy numbers of IL-17 mRNA are approximately 20-30-fold more than those of IFN-γ mRNA in EAM hearts. This is consistent with results involving IFN-γ from previous studies;[21] and absolute copy numbers of IL-17 mRNA measured in this study are approximately 300-fold more than those of IL-2 mRNA obtained from previous data.[21] It has been reported that IL-17-producing $CD4^+$T cells in CNS lesions of EAE behaved similarly to IFN-γ-producing cells but IL-17-producing cells outnumbered IFN-γ-producing cells[31] and that neutralization of IL-17 with a monoclonal antibody ameliorated EAE.[32] Steinman has recently reviewed the roles of Th cells subsets. He proposes that Th1 cells, long thought to mediate tissue damage, might be involved in the initiation of damage but that they do not sustain or play a decisive role in many commonly studied models of inflammation and that a pathway named Th17 is now credited for causing and sustaining tissue damage.[9] IL-23, which is suggested to be responsible for the differentiation and expansion of Th17 cells from naive $CD4^+$T cells,[33] was also expressed in the early phase of EAM and in $CD11b^+$ cells. IL-23 produced by $CD11b^+$ cells, macrophages or dendritic cells and so on might promote IL-17 production in Th17 cells and trigger inflammatory events in hearts.

In this study, it is interesting that IL-10-Ig-containing medium or serum significantly inhibited the gene expression of IL-17 in IL-1-stimulated spleen cells from EAM rats. IL-10 was previously reported to inhibit proinflammatory cytokines such as IL-1β and TNF-α;[34] however, the effects of IL-10 on IL-17 remain unknown. Lubberts et al reported that IL-4 gene therapy for collagen arthritis suppressed synovial IL-17 and improved arthritis.[35] In this study, the IL-10-Ig protein suppressed IL-17 gene expression in IL-1-stimulated spleen cells from EAM rats and improved EAM. This might be similar to their report of the IL-4 effect on IL-17. Recently, it was also reported that IL-23 and not IL-12 was essential for the manifestation of chronic intestinal inflammation by producing the proinflammatory mediators IL-17 and IL-6 in IL-10-deficient mice, which spontaneously developed enterocolitis.[36] IL-10 expression in EAM hearts increased later than IL-17, and the recovery of EAM was concomitant with the increase of IL-10 as well as EAE.[37] Sutton et al reported that IL-23-induced IL-17 production was substantially enhanced by IL-1, and IL-1 functioned upstream of IL-17 to promote pathogenic Th17 cells in EAE.[38] Both IL-1 and IL-23 are strongly expressed in $CD11b^+$ cells in the early phase of EAM, and αβT cells are thought to be strongly stimulated by IL-1 and IL-23; therefore, αβT cells in EAM are thought to express IL-17 strongly. Our data suggests that IL-10 significantly inhibited IL-17 expression in αβT cells under such conditions. Future research needs to consider why IL-10 inhibits IL-17 expression in IL-1-stimulated spleen cells.

In this study, we investigated the alterations of IL-17- and IL-23-producing and -targeting cells in EAM hearts. We demonstrated that IL-10-Ig treatment by a hydrodynamic-based delivery ameliorated EAM, and that IL-10-Ig significantly inhibited IL-17 expression in IL-1-stimulated spleen cells from EAM rats. IL-17 was expressed more highly than Th1 cytokines as IFN-γ or IL-2 in αβT cells in the early phase of EAM hearts. These data suggest that IL-17, produced by Th17, plays an important role in the pathogenesis of EAM and future studies should investigate not only the Th1/Th2 cytokine balance but also the role that Th17 cytokine plays in the development of myocarditis.

Acknowledgments

This work was supported, in part, by grants for scientic research from the Ministry of Education, Culture, Sports, Science and Technology of Japan.

References

1. Kodama M, Matsumoto Y, Fujiwara M. In vivo lymphocyte-mediated myocardial injuries demonstrated by adoptive transfer of experimental autoimmune myocarditis. *Circulation* 1992; **85:** 1918–1926.
2. Kodama M, Zhang S, Hanawa H, Shibata A. Immunohistochemical characterization of infiltrating mononuclear cells in the rat heart with experimental autoimmune giant cell myocarditis. *Clin Exp Immunol* 1992; **90:** 330–335.
3. Hanawa H, Tsuchida M, Matsumoto Y, Watanabe H, Abo T, Sekikawa H, et al. Characterization of T cells infiltrating the heart in rats with experimental autoimmune myocarditis: Their similarity to extrathymic T cells in mice and the site of proliferation. *J Immunol* 1993; **150:** 5682–5695.
4. Seder RA, Paul WE. Acquisition of lymphokine-producing phenotype by CD4+ T cells. *Annu Rev Immunol* 1994; **12:** 635–673.
5. Fuse K, Kodama M, Aizawa Y, Yamaura M, Tanabe Y, Takahashi K, et al. Th1/Th2 balance alteration in the clinical course of a patient with acute viral myocarditis. *Jpn Circ J* 2001; **65:** 1082–1084.
6. Suzuki J, Ogawa M, Futamatsu H, Kosuge H, Tanaka H, Isobe M. A cyclooxygenase-2 inhibitor alters Th1/Th2 cytokine balance and suppresses autoimmune myocarditis in rats. *J Mol Cell Cardiol* 2006; **40:** 688–695.

7. Liu W, Li WM, Gao C, Sun NL. Effects of atorvastatin on the Th1/Th2 polarization of ongoing experimental autoimmune myocarditis in Lewis rats. *J Autoimmun* 2005; **25:** 258–263.
8. Iwakura Y, Ishigame H. The IL-23/IL-17 axis in inflammation. *J Clin Invest* 2006; **116:** 1218–1222.
9. Steinman L. A brief history of T(H)17, the first major revision in the T(H)1/T(H)2 hypothesis of T cell-mediated tissue damage. *Nat Med* 2007; **13:** 139–145.
10. Komiyama Y, Nakae S, Matsuki T, Nambu A, Ishigame H, Kakuta S, et al. IL-17 plays an important role in the development of experimental autoimmune encephalomyelitis. *J Immunol* 2006; **177:** 566–573.
11. Infante-Duarte C, Horton HF, Byrne MC, Kamradt T. Microbial lipopeptides induce the production of IL-17 in Th cells. *J Immunol* 2000; **165:** 6107–6115.
12. Bi Y, Liu G, Yang R. Th17 cell induction and immune regulatory effects. *J Cell Physiol* 2007; **211:** 273–278.
13. Parham C, Chirica M, Timans J, Vaisberg E, Travis M, Cheung J, et al. A receptor for the heterodimeric cytokine IL-23 is composed of IL-12Rbeta1 and a novel cytokine receptor subunit, IL-23R. *J Immunol* 2002; **168:** 5699–5708.
14. Nakae S, Saijo S, Horai R, Sudo K, Mori S, Iwakura Y. IL-17 production from activated T cells is required for the spontaneous development of destructive arthritis in mice deficient in IL-1 receptor antagonist. *Proc Natl Acad Sci USA* 2003; **100:** 5986–5990.
15. Rangachari M, Mauermann N, Marty RR, Dirnhofer S, Kurrer MO, Komnenovic V, et al. T-bet negatively regulates autoimmune myocarditis by suppressing local production of interleukin 17. *J Exp Med* 2006; **203:** 2009–2019.
16. Sonderegger I, Rohn TA, Kurrer MO, Iezzi G, Zou Y, Kastelein RA, et al. Neutralization of IL-17 by active vaccination inhibits IL-23-dependent autoimmune myocarditis. *Eur J Immunol* 2006; **36:** 2849–2856.
17. Watanabe K, Nakazawa M, Fuse K, Hanawa H, Kodama M, Aizawa Y, et al. Protection against autoimmune myocarditis by gene transfer of interleukin-10 by electroporation. *Circulation* 2001; **104:** 1098–1100.
18. Elnaggar R, Hanawa H, Liu H, Yoshida T, Hayashi M, Watanabe R, et al. The effect of hydrodynamics-based delivery of an IL-13-Ig fusion gene for experimental autoimmune myocarditis in rats and its possible mechanism. *Eur J Immunol* 2005; **35:** 1995–2005.
19. Hanawa H, Abe S, Hayashi M, Yoshida T, Yoshida K, Shiono T, et al. Time course of gene expression in rat experimental autoimmune myocarditis. *Clin Sci (Lond)* 2002; **103:** 623–632.
20. Park H, Li Z, Yang XO, Chang SH, Nurieva R, Wang YH, et al. A distinct lineage of CD4 T cells regulates tissue inflammation by producing interleukin 17. *Nat Immunol* 2005; **6:** 1133–1141.
21. Yoshida T, Hanawa H, Toba K, Watanabe H, Watanabe R, Yoshida K, et al. Expression of immunological molecules by cardiomyocytes and inflammatory and interstitial cells in rat autoimmune myocarditis. *Cardiovasc Res* 2005; **68:** 278–288.
22. Chang H, Hanawa H, Liu H, Yoshida T, Hayashi M, Watanabe R, et al. Hydrodynamic-based delivery of an interleukin-22-Ig fusion gene ameliorates experimental autoimmune myocarditis in rats. *J Immunol* 2006; **177:** 3635–3643.
23. Yang S, Li W, Liu W, Gao C, Zhou B, Li S, et al. IL-10 gene modified dendritic cells induced antigen-specific tolerance in experimental autoimmune myocarditis. *Clin Immunol* 2006; **121:** 63–73.
24. Nakano A, Matsumori A, Kawamoto S, Tahara H, Yamato E, Sasayama S, et al. Cytokine gene therapy for myocarditis by in vivo electroporation. *Hum Gene Ther* 2001; **12:** 1289–1297.
25. Kodama M, Matsumoto Y, Fujiwara M, Masani F, Izumi T, Shibata A. A novel experimental model of giant cell myocarditis induced in rats by immunization with cardiac myosin fraction. *Clin Immunol Immunopathol* 1990; **57:** 250–262.
26. Liu H, Hanawa H, Yoshida T, Elnaggar R, Hayashi M, Watanabe R, et al. Effect of hydrodynamics-based gene delivery of plasmid DNA encoding interleukin-1 receptor antagonist-Ig for treatment of rat autoimmune myocarditis: Possible mechanism for lymphocytes and noncardiac cells. *Circulation* 2005; **111:** 1593–1600.
27. Maruyama H, Higuchi N, Nishikawa Y, Kameda S, Iino N, Kazama JJ, et al. High-level expression of naked DNA delivered to rat liver via tail vein injection. *J Gene Med* 2002; **4:** 333–341.
28. Hanawa H, Watanabe R, Hayashi M, Yoshida T, Abe S, Komura S, et al. A novel method to assay proteins in blood plasma after intravenous injection of plasmid DNA. *Tohoku J Exp Med* 2004; **202:** 155–161.
29. Drexler H, Hanze J, Finckh M, Lu W, Just H, Lang RE. Atrial natriuretic peptide in a rat model of cardiac failure: Atrial and ventricular mRNA, atrial content, plasma levels, and effect of volume loading. *Circulation* 1989; **79:** 620–633.
30. Abe S, Hanawa H, Hayashi M, Yoshida T, Komura S, Watanabe R, et al. Prevention of experimental autoimmune myocarditis by hydrodynamics-based naked plasmid DNA encoding CTLA4-Ig gene delivery. *J Card Fail* 2005; **11:** 557–564.
31. Hofstetter HH, Toyka KV, Tary-Lehmann M, Lehmann PV. Kinetics and organ distribution of IL-17-producing CD4 cells in proteolipid protein 139-151 peptide-induced experimental autoimmune encephalomyelitis of SJL mice. *J Immunol* 2007; **178:** 1372–1378.
32. Hofstetter HH, Ibrahim SM, Koczan D, Kruse N, Weishaupt A, Toyka KV, et al. Therapeutic efficacy of IL-17 neutralization in murine experimental autoimmune encephalomyelitis. *Cell Immunol* 2005; **237:** 123–130 (E-publication: 28 Dec 2005).
33. Harrington LE, Hatton RD, Mangan PR, Turner H, Murphy TL, Murphy KM, et al. Interleukin 17-producing CD4+ effector T cells develop via a lineage distinct from the T helper type 1 and 2 lineages. *Nat Immunol* 2005; **6:** 1123–1132.
34. de Waal Malefyt R, Abrams J, Bennett B, Figdor CG, de Vries JE. Interleukin 10(IL-10) inhibits cytokine synthesis by human monocytes: An autoregulatory role of IL-10 produced by monocytes. *J Exp Med* 1991; **174:** 1209–1220.
35. Lubberts E, Joosten LA, Chabaud M, van Den Bersselaar L, Oppers B, Coenen-De Roo CJ, et al. IL-4 gene therapy for collagen arthritis suppresses synovial IL-17 and osteoprotegerin ligand and prevents bone erosion. *J Clin Invest* 2000; **105:** 1697–1710.
36. Yen D, Cheung J, Scheerens H, Poulet F, McClanahan T, McKenzie B, et al. IL-23 is essential for T cell-mediated colitis and promotes inflammation via IL-17 and IL-6. *J Clin Invest* 2006; **116:** 1310–1316.
37. Kennedy MK, Torrance DS, Picha KS, Mohler KM. Analysis of cytokine mRNA expression in the central nervous system of mice with experimental autoimmune encephalomyelitis reveals that IL-10 mRNA expression correlates with recovery. *J Immunol* 1992; **149:** 2496–2505.
38. Sutton C, Brereton C, Keogh B, Mills KH, Lavelle EC. A crucial role for interleukin (IL)-1 in the induction of IL-17-producing T cells that mediate autoimmune encephalomyelitis. *J Exp Med* 2006; **203:** 1685–1691.

BURNS XXX (2008) XXX–XXX

available at www.sciencedirect.com

ScienceDirect

journal homepage: www.elsevier.com/locate/burns

Case report

Mimicking Kawasaki disease in burned children: Report of four cases☆

Takaaki Muro[a,*], *Yu Maruyama*[b], *Kiyoshi Onishi*[a], *Michio Saze*[b], *Emi Okada*[b], *Hiroyuki Matsuura*[c], *Tsutomu Saji*[c]

[a] *Department of Plastic and Reconstructive Surgery, Toho University Ohashi Medical Center, 2-17-6 Ohashi, Meguro-ku, Tokyo 153-8515, Japan*

[b] *Department of Plastic and Reconstructive Surgery, Toho University Omori Medical Center, 6-11-1 Omorinishi, Ota-ku, Tokyo 143-8541, Japan*

[c] *The First Department of Pediatrics, Toho University Omori Medical Center, 6-11-1 Omorinishi, Ota-ku, Tokyo 143-8541, Japan*

ARTICLE INFO

Article history:
Accepted 6 March 2008

1. Introduction

Kawasaki's disease presents with fever, bulbar conjunctival injection, redness of the labial and oral mucosa, polymorphous rashes, changes at the distal ends of the extremities, and cervical lymphadenopathy [2,12]. Complications caused by coronary arterial lesions, which are adverse symptoms, markedly affect the long-term prognosis of patients. When such complications are predicted, high-dose intravenous gammaglobulin therapy is provided from an early stage according to 'Harada's score [8]' which is the most reliable assessment score for the medical treatment of Kawasaki disease in Japan (Table 1). It is a low-incidence disease encountered in the field of Plastic and Reconstructive Surgery, and is considered to occur in more than 100 out of 100,000 children from 0 to 4 years of age in Japan. Although the etiology is unknown, many studies have reported that pathogen-related factors and some additional host factors lead to the development of the disease [19,24,33]. We report four cases with Kawasaki disease, the onset of which was apparently triggered by burns.

2. Case report

Case 1: A 9-month-old boy was consulted to our department with chief complaints of scalds on the right forearm, palm, and lower limb. His past history was unremarkable. He suffered the scalds, developed fevers of 39.0–39.9 °C, and was therefore referred to our department 2 days later. He had superficial dermal burns (SDB) on the right forearm to fingers and on the right thigh to lower leg, and deep dermal burns (DDBs) on the dorsum of the right foot, with a total burn area of 8% (Fig. 1a and b). He was admitted in the hospital the same day, and received fluid and antibiotic (CFPN-PI) therapy and conservative treatment with topical application of amikacin-containing Eksalb® and silver sulfadiazine to the burn wound surface. The patient's general and local condition good, and he was scheduled for skin grafting. However, on the 9th hospital day, he developed a fever of over 40 °C, generalized diffuse erythema, redness at the Bacillus Calmette–Guerin vaccine (BCG) inoculation site, and bulbar conjunctival injection. Hematologic and biochemical tests showed an increased WBC count of 14,400 mm^{-3}, normal red cell and platelet

☆ This article was presented at the 48th Annual Meeting of Japan Society of Plastic and Reconstructive Surgery, 13 April 2005, Tokyo, Japan.

* *Corresponding author.* Tel.: +81 3 3468 1251; fax: +81 3 3468 1264.
E-mail address: muro_logy@yahoo.co.jp (T. Muro).

doi:10.1016/j.burns.2008.03.004

Please cite this article in press as: Muro T, et al., Mimicking Kawasaki disease in burned children: Report of four cases, Burns (2008), doi:10.1016/j.burns.2008.03.004

Table 1 – The guidelines for gammaglobulin application established by the Ministry of Health and Welfare: 'Harada's Score'

Judgment is made based on data obtained by the 9th hospital day in the acute stage

1. WBC: more than 12,000 mm^{-3}
2. Platelet count: less than 350,000 mm^{-3}
3. CRP: more than 3+
4. Hct: less than 35%
5. Albumin: less than 3.5 g/dl
6. Age: 12 months or less
7. Male sex

Cases meeting four or more of these seven items are indicated for gammaglobulin treatment. When the test is performed several times, the lowest values during the course are adopted for assessment.

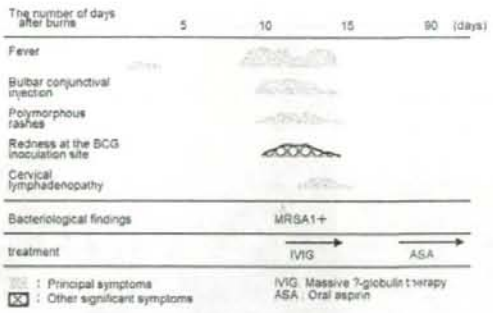

Fig. 2 – Case 1: clinical course.

counts, and evidence of inflammatory reaction and mild liver dysfunction such as a CRP of 5.5 mg/dl, GOT of 47 IU/l, GPT of 77 IU/l, but no abnormalities in BUN, Cr, or CPK. ASO and ASK antibody titers were negative. Urinalysis revealed proteinuria. On the 13th day, cervical lymphadenopathy was noted, and the patient was diagnosed with Kawasaki disease at the Department of Pediatrics of our hospital. He had a Harada score of 5/7 [8], and was immediately started on high-dose intravenous gammaglobulin therapy and oral aspirin, which achieved a complete response. During the course of the disease, no coronary artery aneurysms were observed. Methicillin-resistant *Staphylococcus aureus* (MRSA) was detected in wound-surface cultures. The MRSA was positive for enterotoxin C and TSST-1 production, and was of coagulase II-type strain. Cultures of nasal and pharyngeal secretions and blood were negative. On the 58th day, the wounds epithelialized, and the patient was discharged (Fig. 2).

Case 2: A 1-year-and-1-month-old girl with chief complaints of scalds on the left face, auricle, neck, left anterior chest, back, and right thigh was referred to our department on the second day after suffering scalds. She had a history of infantile asthma. She suffered the scalds, was brought to the emergency room of our hospital, and was referred to our department on the second day after injury. She had superficial burns with deep areas on the thigh, with a total burn area of 20% (Fig. 3a and b), and was hospitalized the same day. She received fluid and topical antibiotic therapy and conservative treatment with topical application of Eksalb® to the burn wound surface. She showed good epithelialization of the wounds; however, she developed fevers of 39–39.9 °C, bulbar conjunctival injection, and lip redness from the 7th day after injury, and generalized erythema, redness at the BCG inoculation site, and strawberry tongue on the 9th day. Hematological and biochemical tests showed an increased WBC count of 17,600 mm^{-3}, increased platelet count of 473,000 mm^{-3}, and evidence of inflammatory reaction and liver dysfunction such as a CRP of 12.6 mg/dl, GOT of 66 IU/l, GPT of 32 IU/l, and LDH of 610 IU/l. ASO, ASK, and EBV-related antibody titers were negative. Urinalysis revealed no abnormalities. On the 10th day, she was diagnosed as having Kawasaki disease at the Department of Pediatrics of our hospital. She had a Harada score of 5/7, and was started on high-dose intravenous gammaglobulin therapy and oral aspirin, with a rapid decline of fever and improvement of other symptoms. From the 17th day, membranous desquamation of the fingers appeared. Though no coronary aneurysm nor other diseases that may cause coronary arterial lesions, such as viral infection and collagen disease-related disorders, developed, Moniliform dilation of the coronary artery was noted during the course. No apparent sign of local infection was noted, but *S. aureus* (MSSA) and MRSA were detected in the wound 8 and 16 days after injury, respectively. The bacteria were TSST-1-producing, enterotoxin C-positive, and coagulase type II. Cultures of nasal and pharyngeal secretions and blood were negative. The wounds epithelialized on the 58th day, and the patient was discharged (Fig. 4).

Case 3: A 10-month-old boy with a chief complaint of scalds on both lower limbs was referred to our department on the

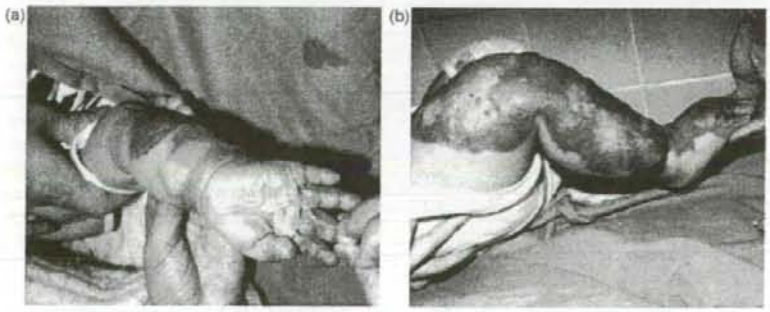

Fig. 1 – (a and b) Case 1: 9-month-old male. Scald burn, SDB-DDB, 8%TBSA.

Please cite this article in press as: Muro T, et al., Mimicking Kawasaki disease in burned children: Report of four cases, Burns (2008), doi:10.1016/j.burns.2008.03.004

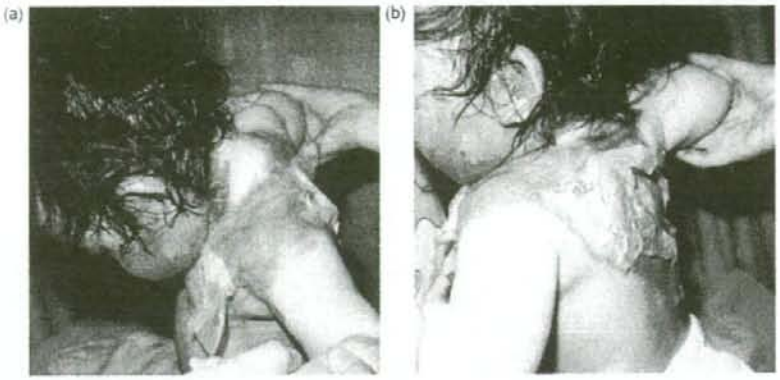

Fig. 3 – (a and b) Case 2: 1-year-and-1-month-old female. Scald burn, SDB-DDB, 20%TBSA.

second day after suffering scalds. His past history was noncontributory. He had superficial burns with deep areas on the dorsum of the feet, with a total burn area of 20%, and was hospitalized the same day. He received fluid and topical antibiotic therapy and conservative treatment with topical application of Eksalb®. He showed good epithelialization of the wounds with no signs of inflammation; however, he developed fevers of over 40 °C, facial and abdominal erythema, redness at the BCG inoculation site, and bulbar conjunctival injection from the 4th day after injury. Hematological and biochemical tests showed an increased WBC count of 24,500 mm^{-3} and evidence of inflammatory reaction and mild liver dysfunction such as a CRP of 10.1 mg/dl, GOT of 37 IU/l, GPT of 20 IU/l, and LDH of 699 IU/l. Urinalysis revealed no abnormalities. Based on the clinical course, atypical Kawasaki disease was diagnosed at the Department of Pediatrics of our hospital. The patient, placed on fluid therapy and topical ointment therapy, achieved symptomatic relief of Kawasaki disease. No coronary aneurysms were noted during the course of the disease. On the 22nd day after injury, membranous desquamation of the fingers appeared. In the absence of evidence of wound infection, MRSA was detected in wound cultures performed on the 9th day after injury, but blood cultures were negative. On the 26th day after injury, he was discharged, and the wounds epithelialized on the 40th day (Fig. 5).

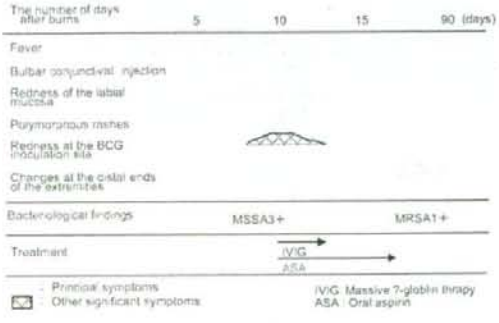

Fig. 4 – Case 2: clinical course.

Case 4: A 2-year-and-2-month-old girl was referred to our department with chief complaints of burns on the right palm and forearm. Her past history was noncontributory. She suffered hot iron contact burns, received conservative treatment at a local clinic, with no improvement, and was referred to our department on the 18th day after injury. She had superficial burns but deep in part, with a total burn area of 0.5%. After hospitalization, she received conservative treatment with topical application of Eksalb®. However, from the 19th day after injury, she had five symptoms of Kawasaki disease such as fevers of over 40 °C and generalized erythema, except for changes at the distal ends of the extremities, and was diagnosed with Kawasaki disease at the Department of Pediatrics of our hospital. She was immediately started on high-dose intravenous gammaglobulin therapy and oral aspirin, and rapidly achieved symptomatic improvement. No coronary aneurysms were noted during the course of the disease. On the 20th day after injury, MRSA was detected in the wounds, which epithelialized on the 48th day (Fig. 6).

3. Discussion

Kawasaki's disease was proposed as a vasculitis of unknown origin by Kawasaki et al. [12]. Kawasaki's disease is defined as a set of five or more of the following six symptoms, or a set of four symptoms in combination with proven coronary aneurysm in the absence of other possible diseases: (1) fever, (2) bulbar conjunctival injection, (3) redness of the labial and oral mucosa, (4) polymorphous rashes, (5) changes at the distal ends of the extremities, and (6) cervical lymphadenopathy. Other significant clinical and laboratory features include heart disease, including coronary artery aneurysm, respiratory and digestive symptoms, leukocytosis with left shift, hypoalbuminemia, anemia, redness at the BCG inoculation site, and neurological symptoms [2]. The incidence is high (68.0%) in infants younger than 3 years of age, 11.1% at 5 years of age or older, and very rare at 20 years of age or older in Japan [11]. The incidence of cardiac complications is about 20% in children and 13.6% in adults [28]. In some cases of Kawasaki's disease, the etiology of which is unknown by definition, potential

Please cite this article in press as: Muro T, et al., Mimicking Kawasaki disease in burned children: Report of four cases, Burns (2008), doi:10.1016/j.burns.2008.03.004

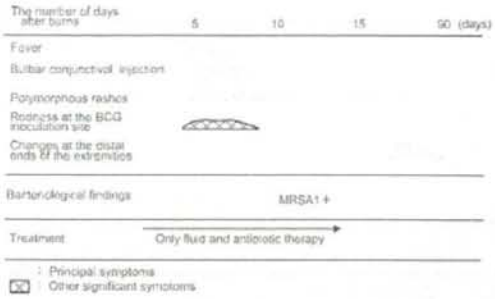

Fig. 5 – Case 3: clinical course.

causative pathogens, substances, or specific antibodies of other inflammatory diseases are detected, or other diseases precede the onset. The disease has many similarities to hemolytic streptococcal infection and measles, and epidemiologically exhibits onset seasonality and regional epidemicity, providing a basis for suspecting the involvement of pathogenic microorganisms as causative agents. Indeed, for the past 30 years, researchers have reported many cases of similar diseases [9,10,13,14,16,19,22–24,26,31–34] (Table 2). Therefore, the terms Kawasaki-like disease or mimicking Kawasaki disease are used to refer to a pathological condition which meets the diagnostic criteria for Kawasaki disease that is caused by an identified pathogen [23]. All the four patients reported here presented with characteristic symptoms meeting the diagnostic criteria for Kawasaki disease, and one of them showed moniliform dilatation of coronary arteries. In addition, antibiotics were ineffective, and high-dose intravenous gammmaglobulin therapy rapidly relieved the symptoms. These results indicate that three of them had typical Kawasaki's disease. However, since these patients developed symptoms after MRSA infection following burns, the condition was diagnosed as mimicking Kawasaki disease.

Recent studies suggested the involvement of infectious agents in the etiology of Kawasaki disease. Saji et al. indicated that Kawasaki disease itself should be understood as a syndrome presenting with similar symptoms [23]. Kawasaki's disease is also characterized by the development of coronary artery aneurysms due to coronary arteritis, an important factor influencing the long-term prognosis. Coronary arteritis

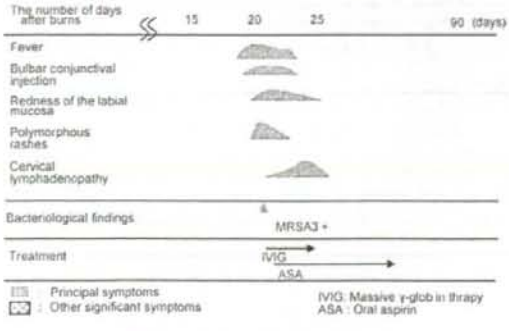

Fig. 6 – Case 4: clinical course.

Table 2 – Causes/diseases reported as mimicking Kawasaki disease

1. Infection (specific inflammatory diseases)
Yersinia
Streptococcus pyogenes
Staphylococcus aureus (TSS, NTED, etc.)
Virus
Measles
Influenza
HIV
EBV
Candida albicans
Mycoplasma
Rickettsiosis
Others
2. Nonspecific inflammatory diseases
After vaccine inoculation (Measles, smallpox and DPT)
After burns
After cellulitis
Insect bite
Systemic rheumatoid arthritis
Infantile periarteritis nodosa
Stevens–Johnson syndrome
Hemophagocytosis syndrome
Henoch–Schonlein purpura
Drug sensitivity
Carbamazepine, mesalazine
Acetoaminophen

or the resulting aneurysms have been reported in 72.5% of childhood vasculitides seen in diseases except Kawasaki disease, such as EB virus-related diseases [20]. The causes that induce childhood coronary arterial complications include EB virus infection described above, nodular periarteritis, and other viral and collagen disease-related disorders. In adults, only arteriosclerotic lesions and systemic lupus erythematosus (SLE) are known as the causes. However, the current International understanding of Kawasaki disease is that the classification of vasculitides includes Kawasaki disease in "primary vasculitides", and distinguishes it from secondary vasculitides related to infections, collagen disease, drug hypersensitivities, cryoglobulinemia, malignant neoplasms, hypocomplementemic urticaria, or transplantation, and post-transplant vasculitis and pseudovasculitis, of which the causes or predisposing causes are present [15].

To our knowledge, there have been only two reported cases of Kawasaki disease that developed after burns [33], excluding our patient, and no adult case has been reported. These cases and ours had the same clinical features: (1) age at onset less than 3 years, (2) burns on relatively small areas of the body, and (3) early onset after burn injury. In general, milder burns epithelialize without becoming infected, whereas deep burns take 3–4 weeks to epithelialize, increasing the chance of infection. All our patients had DDB in all or part of the burn surface, and developed Kawasaki disease during burn wound infection. Kawasaki disease tends to develop at about 1 year of age when passive immunity from the mother declines, a fact also consistent with the observations in our patients. The development of Kawasaki disease in association with burns on relatively small areas of the body suggests the involvement of various factors. Extensive burns are often treated early by massive fluid therapy, antibiotic therapy, and anti-shock

Please cite this article in press as: Muro T, et al., Mimicking Kawasaki disease in burned children: Report of four cases, Burns (2008), doi:10.1016/j.burns.2008.03.004